Bias Assessment and Data Drift Detection in Medical Image Analysis: A Survey

Anonymous authors
Paper under double-blind review

Abstract

Machine learning (ML) models have achieved expert-level performance across a range of diagnostic tasks in medical image analysis, yet their adoption in clinical practice remains limited due to concerns over reliability, fairness, and robustness. Two key threats to trustworthy deployment are bias, arising primarily during model development, and data drift, which occurs post-deployment as data distributions change over time. Although conceptually distinct, these two phenomena are often conflated in the literature or addressed in isolation, despite their potential to interact and jointly undermine model performance. We argue that clearly distinguishing between bias and data drift is essential for developing appropriate reliability strategies: methods designed to mitigate bias during training differ fundamentally from those needed to detect and manage drift in deployment. In this survey, we therefore bring these perspectives together within a unified framework, clarifying their boundaries while also highlighting where they intersect. We present a comprehensive review of methods for assessing and monitoring ML reliability in medical image analysis, focusing on disease classification models. We first define and distinguish bias and data drift, illustrate their manifestations in clinical contexts, and categorise their sources. We then review state-of-the-art approaches for bias encoding assessment and data drift detection, as well as methods for estimating model performance degradation when ground truth labels are not immediately available. Our synthesis highlights methodological gaps, particularly in evaluating drift detection techniques on real-world medical data, and outlines open challenges for future research. By consolidating these perspectives and providing accessible explanations for both technical and clinical audiences, this work aims to support collaboration between developers, clinicians, and healthcare institutions in building fair, transparent, and reliable ML systems for clinical use.

1 Introduction

In recent years, technological and algorithmic advances have enabled machine learning (ML) models to achieve expert-level performance in a range of diagnostic and prognostic tasks across medical imaging modalities (Banerjee et al., 2023). From identifying tumors in radiological scans to predicting cardiovascular risks in ultrasound imaging, these models have shown considerable promise as clinical decision support tools (Jones et al., 2023). However, despite this potential, their integration into routine clinical practice remains limited (Salahuddin et al., 2022). A key barrier to adoption is the lack of robustness and trustworthiness across diverse patient populations and clinical environments required for real-world deployment in safety-critical healthcare environments (Saw & Ng, 2022).

Two central challenges to achieving reliable ML in medical image analysis are bias and data drift. Bias typically arises during model development when training data fail to capture the heterogeneity of the target population. For example, models trained predominantly on adult imaging data may underperform on pediatric cases due to anatomical and physiological differences. Additionally, systemic disparities in healthcare access can result in the underrepresentation of certain demographic groups in training sets (DeBenedectis et al., 2022), leading to a degraded model performance for these groups (Seyyed-Kalantari et al., 2020; 2021).

Such biases risk perpetuating or exacerbating existing healthcare inequities (Obermeyer et al., 2019; Char et al., 2018; Gianfrancesco et al., 2018; Glocker et al., 2023a).

In contrast, data drift refers to changes in the input data distribution that occur between model training and deployment (Sahiner et al., 2023). These shifts may be abrupt or gradual, and can stem from variations in imaging hardware, acquisition protocols, patient demographics, or clinical workflows (Kore et al., 2024). For instance, a model developed using data from one hospital may fail when applied in another setting with different equipment or population characteristics. Even within a single hospital, shifts in patient composition (*e.g.* during a pandemic) or the introduction of new scanners can lead to data drift, degrading model performance in ways that often go undetected until clinical harm occurs (Duckworth et al., 2021).

Although conceptually and operationally distinct, bias and data drift are closely linked through their shared impact on model reliability, a prerequisite for safe clinical deployment. Nevertheless, they are rarely addressed together in the literature and are frequently conflated in terminology and scope. Bias arises from static conditions in data curation and model development (pre-deployment), whereas data drift manifests dynamically in deployed systems facing evolving clinical environments (post-deployment). Consequently, mitigation strategies differ: bias requires fair data collection and algorithmic fairness methods, while data drift necessitates ongoing monitoring and model recalibration or retraining (Kore et al., 2024).

Despite their critical importance, no unified framework currently delineates bias and data drift in a systematic way. Existing studies often address them interchangeably, without making their distinction explicit (Drukker et al., 2023; Vrudhula et al., 2024; Tejani et al., 2024; Koçak et al., 2025; Hasanzadeh et al., 2025). Other works focus narrowly on one dimension, either data drift (Gama et al., 2014; Kore et al., 2024) or bias (Brown, 2017; Puyol-Antón et al., 2021; Stanley et al., 2024a), or even just on a single facet of one of them (Omar et al., 2025; Godau et al., 2025; Abdullahi et al., 2025). Yet considering bias and data drift in isolation is inadequate for developing reliable ML systems, as the two can interact in subtle but consequential ways. For instance, drift within already underrepresented subgroups may remain undetected when performance is assessed only at the population level, allowing existing biases to mask the emergence of data drift (Khoshravan Azar et al., 2023). As shown in Figure 1, these phenomena emerge at different stages of the ML lifecycle but jointly determine a model's reliability in real-world deployment.

Motivated by these challenges, this survey brings together both topics, bias and data drift, in a unified review focused on reliability in medical image analysis. By addressing both phenomena side-by-side, we aim to clarify their definitions, differentiate their causes and implications, and survey existing methodologies for detecting and mitigating their effects. Moreover, our review is positioned to bridge the gap between technical and clinical communities: we intentionally use accessible language and illustrative examples to make these concepts understandable to readers with limited background in computer science or machine learning. This is essential in an interdisciplinary field where close collaboration between developers, clinicians, but also research and healthcare institutions is vital.

The key contributions of this work are as follows:

- We establish precise and operational definitions of *bias* and *data drift*, clarifying their distinct roles in the context of machine learning (ML) reliability for medical image analysis.
- Concepts are presented in accessible language to engage both technical and clinical audiences, minimizing reliance on domain-specific jargon.
- Illustrative examples from the medical domain demonstrate how bias and data drift manifest in real-world clinical settings.
- A structured taxonomy is proposed to categorize sources of bias and data drift, including patient-, device-, and workflow-level factors.
- We review current methods for detecting and mitigating bias in medical image analysis, with particular focus on fairness and representational adequacy.
- State-of-the-art techniques for identifying and quantifying data drift are surveyed, emphasizing their relevance for maintaining clinical model performance.
- We highlight key challenges and open research questions, outlining opportunities to improve the fairness, robustness, and long-term reliability of clinical ML systems.
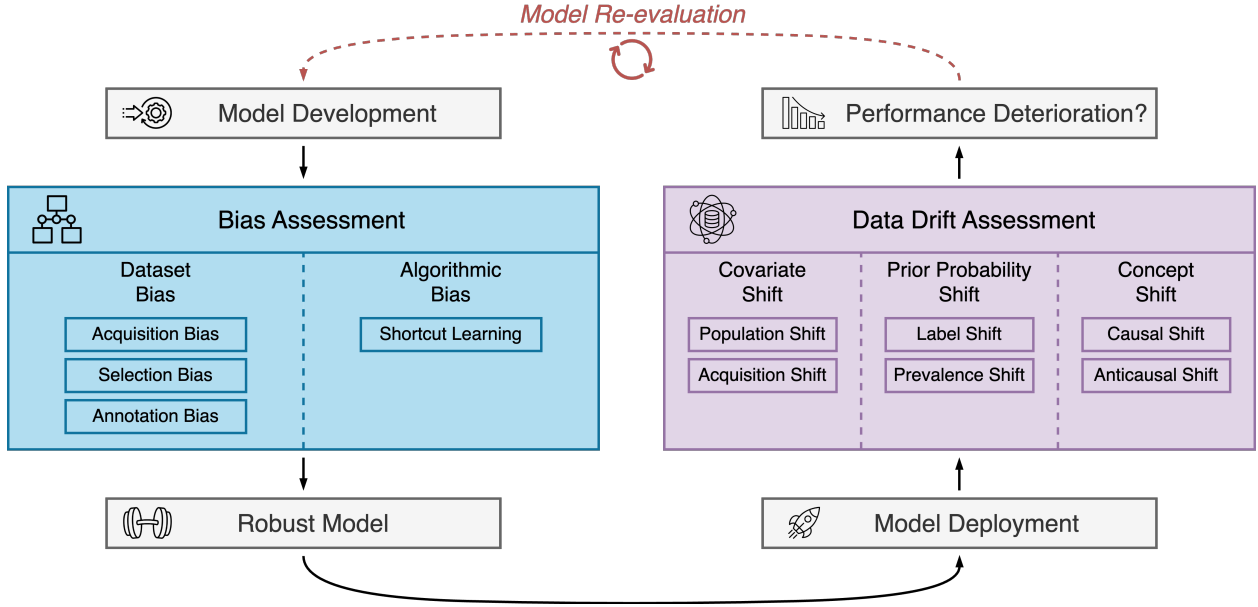
Figure 1: Reliability assessment lifecycle for machine learning models in medical image analysis, showing that bias assessment occurs during model development and data drift assessment during deployment when the model faces evolving clinical environments. Bias is categorized into dataset bias including acquisition, selection and annotation bias, and algorithmic bias such as shortcut learning. Data drift is categorized into covariate shift (population shift, acquisition shift), prior probability shift (label shift, prevalence shift) and concept shift (causal shift, anticausal shift). This taxonomy is used throughout the paper to distinguish bias and data drift and to highlight their distinct but complementary roles in ensuring robustness, fairness and long term reliability of clinical ML systems.

The remainder of this paper is organized as follows. Section 2 introduces the key concepts of bias, including its implications, types, and associated assessment metrics and challenges. Section 3 presents the main concepts of data drift, its clinical relevance, and assessment approaches, along with the inherent challenges in evaluation. Sections 4 and 5 review state-of-the-art methods for bias encoding assessment and data drift detection, respectively. Finally, Section 6 provides an integrated discussion of findings, and Section 7 concludes with open research challenges and future directions.

2 Key Concepts of Bias

Bias refers to an estimate of a statistic being systematically different from its population value. If estimates were unbiased on the population level, models would generalise well to other datasets (Wachinger et al., 2019). In the context of ML, we follow recent literature (Seyyed-Kalantari et al., 2020; Brown et al., 2023) and define bias as performance disparities across defined subgroups, such as those distinguished by race, age, or gender (Cheong et al., 2023). These attributes are commonly referred to as *sensitive attributes*, as they are associated with socially or clinically meaningful categories that should not unjustifiably affect algorithmic outcomes.

Understanding the causal structure between features and outcomes is essential for identifying and addressing bias. In a *causal* relationship, the input variable X (*e.g.* an image) influences the label Y (*e.g.* diagnosis); this is the typical setting assumed in most supervised learning tasks. In contrast, an *anticausal* relationship occurs when Y is the true causal driver of X, such as when disease status causes observable changes in imaging. Many medical tasks are inherently anticausal, which complicates bias detection and mitigation, as correlations between sensitive attributes and X or Y may reflect underlying structural or social confounding rather than spurious noise.

Although identifying the source of bias is essential for selecting the appropriate bias mitigation strategies (Cheong et al., 2023), it is a non-trivial task. Contributing to this difficulty are the complexity of high-dimensional statistical functions (*e.g.* ML models), the entanglement of multiple sources of bias (Koçak et al., 2024), and the presence of unobservable confounding factors in the data (Cheong et al., 2023). Słowik & Bottou (2021) outline two sides to the bias debate: one focuses on *data*, and the other one focuses on *algorithms*. We adhere to this distinction, and in the remainder of this section (*cf.* Sections 2.1–2.2), we contextualise these challenges specifically within the medical domain.

2.1 Dataset Bias

A dataset can be conceptualised as a finite, and potentially biased, sample drawn from the true joint probability distribution of the real world, denoted as $P_{REAL}(X, Y)$, where $P_{REAL}(X)$ represents the distribution over input samples (*e.g.* medical images), and $P_{REAL}(Y)$ represents the distribution over corresponding labels (*e.g.* diagnostic annotations). Ideally, a dataset is considered unbiased if its empirical joint distribution $P_{MODEL}(X, Y)$ closely mirrors $P_{REAL}(X, Y)$. However, in practice, sampling is influenced by selection mechanisms, *e.g.* of clinical, demographic, or technical nature, that determine which instances are included in the dataset. These mechanisms can lead to deviations in $P_{MODEL}(X)$ from $P_{REAL}(X)$. Furthermore, when annotations are involved, the process of assigning labels, whether through human judgment or algorithmic heuristics, can distort the conditional distribution $P_{MODEL}(Y|X)$. This introduces annotation bias, whereby the observed labels systematically deviate from the true labels, particularly if certain subpopulations are mislabelled more frequently (Cheong et al., 2023).

Consequently, bias in the dataset, reflected in the misalignment between $P_{MODEL}(X, Y)$ and $P_{REAL}(X, Y)$, can arise from two main sources: the input distribution X, due to selective sampling, and the label distribution Y, due to annotation errors. Thus, the resulting dataset encodes not only information about the real world, but also the imperfections and asymmetries of the processes used to collect and label the data.

Figure 2: Graphical models illustrating (a) Selection Bias: A selection mechanism C (*e.g.* which gets included in the dataset) is influenced by both sensitive attribute S and label Y, which then influences the input X, and (b) Annotation Bias: The observed label $\bar{Y}$ is affected by both the true label Y and the sensitive attribute S, introducing systematic errors into the ground truth. The error in the observed label $\bar{Y}$ can influence the selection of input X.

2.1.1 Acquisition bias

Acquisition bias is a persistent challenge in medical imaging, arising from systematic variability in how images are captured across institutions, or even within the same healthcare facility over time. This form of bias affects the input distribution $P_{MODEL}(X)$ and can undermine downstream model generalisability when acquisition characteristics are not adequately represented or harmonised.

A primary source of acquisition bias is domain shift (Guan & Liu, 2021), which arises from differences in scanner hardware and imaging protocols. For instance, T1-weighted MRI scans acquired from the same patient can exhibit notable differences in contrast and brightness when obtained using scanners from different manufacturers, models, or deployment sites (Opfer et al., 2023). Similarly, in digital pathology, variability in staining protocols, scanner types, compression methods, and optical settings introduces substantial distribution shifts (Madabhushi & Lee, 2016; Dimitriou et al., 2019). To this extent, these acquisition-related biases should be documented using standardised tools such as datasheets for datasets (Mbakwe et al., 2023).

Although acquisition differences may appear purely technical, they can lead to structural confounding when specific patient groups are consistently imaged using particular scanners or protocols associated with certain hospitals or regions.

2.1.2 Selection Bias

Dataset bias regarding the input X can result from selection bias (Wachinger et al., 2019), see Figure 2(a). The selection mechanism C of samples can be influenced by a sensitive attribute and the label Y. This can arise when the participants included in the study do not accurately represent the overall population (Wachinger et al., 2019), *e.g.* when a specific subgroup is over- or under-represented compared to others (Banerjee et al., 2023). Selection bias in clinical practice is evident when, *e.g.* radiologic images are frequently collected from just one or a few locations, resulting in a lack of geographic and racial diversity. Additionally, systemic disparities can lead to variations in image quality, with *e.g.* Black and Hispanic patients sometimes receiving lower quality and less advanced imaging for similar symptoms in emergency departments, especially in patient cost-driven settings like the US (DeBenedectis et al., 2022).

Selection bias can lead to severe class imbalance causing ML models to predominantly learn from the majority class. As a result, these models tend to achieve high performance metrics for the that class, but fail to generalise effectively to any minority classes (Banerjee et al., 2023). Similar challenges occur with demographic factors like gender and socio-economic status, where ML models tend to perform more effectively for the demographic groups that are disproportionately over-represented in the training data (Koçak et al., 2024). Notably, there is no universally robust training set. Although the training distribution is representative of the actual test distribution, the trained model may still perform poorly on certain subgroups. In case of a classification problem, this can be caused by the majority and minority population having different classification boundaries (Słowik & Bottou, 2021).

2.1.3 Annotation Bias

Label bias, or annotation bias, arises from significant variability among annotators when classifying or delineating regions of interest in diseased areas on data like medical images (Banerjee et al., 2023). As illustrated in Figure 2(b), a sensitive attribute S can influence the annotation process so that the observed label $\bar{Y}$ differs from the ground truth label Y. Annotation shift, where certain subgroups may be systematically mislabelled more frequently than others, *e.g.* underdiagnosis of conditions in minority populations or tending to assign positive labels for ambiguous findings in elderly patients as in breast cancer screening (Autier et al., 2017), can introduce subgroup-specific inconsistencies potentially leading to annotation bias. In case of annotation shift, the model is unlikely to perform well across different subgroups, as the relationship between disease labels and imaging features becomes inconsistent (Bernhardt et al., 2022).

2.2 Algorithmic Bias

Apart from training data, model design plays a crucial role with respect to bias amplification. Algorithms are not impartial, and certain design choices lead to fairer prediction outcomes (Hooker, 2021). In general, ML systems that focus on minimising average error have been found to perform inconsistently across significant subsets of the data. Optimising for the loss averaged over the entire population can easily result in models that perform poorly on specific subpopulations (Słowik & Bottou, 2021). Model design choices aimed at maximising test-set accuracy often fail to preserve other important properties, such as robustness and fairness. One key reason these choices amplify algorithmic bias is that fairness often coincides with how the model treats underrepresented protected features. The algorithmic bias a model acquires can be linked to the disproportionate over- or underrepresentation of a protected attribute within a specific category. Identifying which model design choices disproportionately increase error rates for protected, underrepresented features is a critical first step in reducing algorithmic harm (Hooker, 2021). Hooker et al. (2020; 2019) found that compression techniques like quantisation and pruning disproportionately impact low-frequency attributes such as age and gender in order to maintain performance on the most frequent features. Jiang et al. (2020) demonstrated that difficult and underrepresented features are learned later in the training process and that the learning rate influences what the model learns. Therefore, early stopping and similar hyperparameter

choices disproportionately affect a subset of the data distribution. Some model design choices are better than others regarding fairness considerations. For instance, with the widespread use of compression and differential privacy techniques in sensitive areas like healthcare diagnostics, understanding the error distribution is crucial for assessing potential harm. In such settings, pruning or gradient clipping may be unacceptable due to their impact on human well-being (Hooker, 2021). A special case of algorithmic bias is stemming from shortcut learning, which is described in more detail in the subsequent section 2.2.1.

2.2.1 Shortcut Learning

Shortcut learning or confounding bias emerges when ML models rely on confounding variables to derive predictions (Boland et al., 2024).

Spurious features can lead to shortcut learning, where ML models depend on superficial or irrelevant features. These features are simple for the model to learn but do not generalise beyond the training data, where the connection between the label Y and the spurious feature S no longer holds, leading to a drop in performance after deployment, see Figure 3. In these cases models may depend on spurious features even when they are less predictive than clinically relevant features (Boland et al., 2024). For instance, ML models relying on portable Intensive Care Unit (ICU) radiographic markers as proxies for the condition rather than identifying the true underlying pathology for pneumonia prediction (Zech et al., 2018) or pneumothorax detection models relying on inserted chest tubes for prediction (Rueckel et al., 2020).
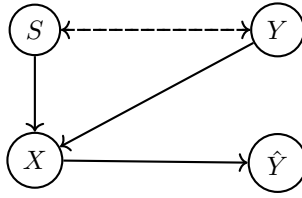

Figure 3: Graphical model for shortcut learning: input X depends on both sensitive attribute S and label Y, while prediction $\hat{Y}$ depends on X. The dashed bidirectional edge between S and Y indicates potential correlation in the dataset (*e.g.* age correlated with disease prevalence), which may lead the model to rely on S as a shortcut for predicting Y, rather than learning clinically meaningful features.

Conversely, ML models might use sensitive attributes S, such as age, sex, or race, to enhance performance, which could be justifiable when these attributes are correlated with disease risk in the target population. For instance, melanoma is more common in lighter skin tones, breast cancer is more prevalent in women, and androgenetic alopecia is more common for men. In these situations, disregarding or removing attribute information could reduce clinical performance (Brown et al., 2023).

Figure 4: Graphical models showing relationships between sensitive attributes (S), data (X), labels (Y), and predictions ($\hat{Y}$)(Dehdashtian et al., 2024). Scenario (a): S and Y are dependent (*e.g.* age affects both label and data). Scenario (b): S and Y are independent (correlation is spurious).

Figure 4 represents the two distinct scenarios of biases relating to sensitive attributes. In Figure 4(a), Y and S are inherently dependent, *e.g.* an attribute like age can influence both the risk of developing a condition and the appearance of the image. A model might learn to predict the presence of a condition based on the attribute. However, this scenario will introduce a trade-off between performance and fairness. In Figure 4(b), Y and S are independent. According to Dehdashtian et al. (2024), any observed correlation can be considered

as spurious correlation, where these correlations are not considerably beneficial for the performance of the model. In scenario (b), the performance of a bias-free model regarding Y being independent of S is expected.

From an ML perspective, biases can be understood as arising from dependencies between data attributes (confounding variables). The data X depends on the target attribute Y and the sensitive attribute S. Bias mitigation aims to guarantee that the prediction $\hat{Y}$ is statistically independent of S. To grasp the effects of biases, it is useful to distinguish between demographic and non-demographic biases. Demographic biases arise when models perform differently across various demographic groups, which can be defined by attributes like gender, race, or age. Ideally, a bias-free model should exhibit consistent performance regardless of these attributes (Dehdashtian et al., 2024). In case of a correlation between S and Y, a performance-fairness trade-off is introduced. Non-demographic biases, *e.g.* measurement artefacts (motion artefacts in MRI), are unrelated to demographic factors (Spisak, 2022). These biases involve spurious correlations that computer vision systems can learn to solve a task. Although these biases are not tied to specific attributes, such attributes may often be identified in various tasks (Dehdashtian et al., 2024).

2.3 Metrics for Bias Assessment

Model fairness is commonly assessed through two principal frameworks: *individual fairness*, which emphasizes consistency at the instance level (Dwork et al., 2012), and *group fairness*, which evaluates outcomes across demographic or social subgroups (Barocas et al., 2023). In the context of group fairness, model behaviour is typically formalised using three core statistical criteria, each of which captures a distinct conditional independence relationship among the predicted outcome $\hat{Y}$, the true label Y, and a sensitive attribute S:

- *Independence* ($\hat{Y} \perp\!\!\!\perp S$) requires that the prediction be uncorrelated with group membership. This criterion reflects equality of outcomes across groups, regardless of the ground truth label.

- *Separation* ($\hat{Y} \perp\!\!\!\perp S \mid Y$) requires that predictions be conditionally independent of sensitive attributes given the true label, ensuring equal error rates across groups.

- *Sufficiency* ($Y \perp\!\!\!\perp S \mid \hat{Y}$) requires that, for any given predicted label, the likelihood of the true label given a predicted label is consistent across groups, reflecting equal predictive value.

Each criterion corresponds to a class of fairness metrics that capture specific types of statistical dependencies (Marcinkevics et al., 2022; Castelnovo et al., 2022). For instance, the *Statistical Parity Difference* (SPD) (Savani et al., 2020), defined in Equation 1, measures the difference in the rates of positive predictions across groups, irrespective of ground truth. This metric operationalises the independence criterion, as it requires prediction rates to be equal across groups regardless of the true label.

$$SPD = P(\hat{Y} = 1 \mid S = 0) - P(\hat{Y} = 1 \mid S = 1) \tag{1}$$

The *Equality of Opportunity Difference* (EOD) (Hardt et al., 2016; Savani et al., 2020), formalised in Equation 2, quantifies the discrepancy between the True Positive Rates (TPRs) of a classifier across groups defined by the sensitive attribute S (Marcinkevics et al., 2022). A significant TPR disparity indicates that individuals with a disease within a protected subgroup are not receiving correct diagnoses at the same rate as the general population, even if the algorithm has a high overall accuracy (Boland et al., 2024). EOD formalizes a relaxed form of separation by focusing only on the positive class ($Y = 1$), thereby enforcing equal true positive rates across groups.

$$EOD = P(\hat{Y} = 1 \mid Y = 1, S = 0) - P(\hat{Y} = 1 \mid Y = 1, S = 1) \tag{2}$$

The *Predictive Parity Difference* (PPD), defined in Equation 3, measures the deviation from the predictive parity condition, which requires equal Positive Predictive Value (PPV) across groups (Chouldechova, 2017). This condition is a relaxed instance of the broader *sufficiency* criterion, which also encompasses equality of Negative Predictive Value (NPV) across groups.

$$PPD = P(Y = 1 \mid \hat{Y} = 1, S = 0) - P(Y = 1 \mid \hat{Y} = 1, S = 1) \tag{3}$$

Disparities in PPD indicate that the model's positive predictions are not equally trustworthy across groups, which can be critical when decisions depend directly on predicted outcomes. Notably, in clinical settings where false negatives carry significant consequences, *e.g.* ruling out cancer, ensuring parity in NPV may be just as important as PPV. For a more comprehensive list of metrics, we refer the reader to related surveys (Verma & Rubin, 2018; Castelnovo et al., 2022; Rabonato & Berton, 2024).

2.4 Challenges in Bias Assessment

The three foundational fairness criteria (*i.e.* independence, separation, and sufficiency) are notably mutually incompatible (Castelnovo et al., 2022; Barocas et al., 2023; Gao et al., 2024). As illustrated in Example 2.1, satisfying one often necessitates violating another, particularly when the predicted outcome $\hat{Y}$, true label Y, and sensitive attribute S exhibit complex statistical dependencies. As a result, fairness assessment is inherently context-dependent and must consider which kinds of errors are more harmful in the specific application domain.

Notably, disease prevalence often correlates with demographic variables such as age, sex, or ethnicity, making rigid notions of group-level equality problematic in clinical applications (Gao et al., 2024). In such cases, enforcing fairness criteria like independence ($\hat{Y} \perp\!\!\!\perp S$), which requires prediction rates to be equal across groups, can lead to clinically inappropriate decisions, as it disregards meaningful and medically justified differences in disease prevalence between groups. As such, defining fairness purely in terms of "equality" may be misleading (Liu et al., 2023). Compounding this, many medical imaging datasets lack adequate socio-demographic representation, limiting the ability to assess bias comprehensively, particularly in intersectional subgroups (Stanley et al., 2023). Moreover, subgroup choice itself plays a critical role in the effectiveness of fairness interventions (Alloula et al., 2025). In some cases, mitigation strategies based on observed disparities within a particular set of subgroups can paradoxically worsen outcomes. Lastly, fairness metrics can be sensitive to distribution shifts, making their behaviour unstable over time and further complicating their interpretation in real-world, dynamic settings (Mienye et al., 2024). Together, these factors highlight the need for fairness frameworks in healthcare that are context-aware, data-driven, and aligned with both clinical utility and ethical considerations.

Example 2.1: Fairness Trade-Off

In breast cancer screening, models are often evaluated on their ability to detect cancer early. Suppose the model achieves equal true positive rates (TPRs) across racial groups, **satisfying Equality of Opportunity (EOD)**, a separation-based metric. This ensures that all women who have cancer are equally likely to be correctly identified, regardless of race.

However, achieving this may require lowering the decision threshold for groups with historically lower TPRs, which can increase false positive rates. As a result, the Positive Predictive Value (PPV), *i.e.* the likelihood that a positive prediction truly reflects cancer, may differ across groups. This **violates the Predictive Parity Difference (PPD)**, a sufficiency-based criterion.

In this case, prioritizing EOD reflects a clinical choice to reduce underdiagnosis, accepting a potential increase in overdiagnosis. This trade-off is often justified in high-risk screening contexts where missing a diagnosis is more harmful than additional follow-up testing.

2.5 Relevance of Bias Assessment in Clinical Practice

Bias in machine learning models has direct consequences beyond statistical fairness, particularly in sensitive domains like healthcare. Indeed, when models perform unequally across demographic groups, they can lead to unequal access to diagnosis or treatment (Obermeyer et al., 2019; Cross et al., 2024). An extensive review on bias types and examples in cardiovascular imaging (Vrudhula et al., 2024) can serve as a useful reference for understanding how such biases manifest in practice and the mechanisms through which they propagate into clinical decision-making.

Consequently, bias affects clinical workflows and outcomes, thereby reinforcing existing health inequalities. Recognising these implications highlights the importance of bias evaluation and mitigation as essential steps toward safe, fair, and robust deployment of ML systems.

3   Key Concepts of Data Drift

In spite of an early effort to standardize the terminology regarding dataset shift (Moreno-Torres et al., 2012), there are still multiple terms used for the same concept across literatures. These terms include domain drift, distributional shift, and dataset shift, among others (Sahiner et al., 2023).

In this section, we first formalize a simplified mathematical definition of data drift. The subsequent subsections outline the motivation behind addressing the problem of data drift and the reason for the occurrence of data drift. Next, we provide insights into the different types of data drift.

The implicit assumption underlying all supervised ML techniques is that the training dataset distribution $P_{TRAIN}(X,Y)$ is the same as the distribution of the data processed by the model post-deployment $P_{DEPLOYED}(X,Y)$. In this context, we define $X \in R^n$ as the vector representation of a data item's covariates and Y its corresponding target variable (Dreiseitl, 2022). Dataset shift occurs when this assumption no longer holds, that is, there occurs a discrepancy in the joint distribution of inputs and outputs (target variables) between the training and deployment stage (Quiñonero-Candela et al., 2022) or when data changes slowly over time because of systematic errors or random population shifts. Specifically, that is the case when $P_{TRAIN}(X,Y) \neq P_{DEPLOYED}(X,Y)$.

Generally, dataset shift can be assumed whenever there are disparities between the distributions of the training and unseen data (Moreno-Torres et al., 2012). (Moreno-Torres et al., 2012) specifies the case of sample selection bias causing dataset shift, where the aforementioned distribution discrepancies arise because the training examples were obtained through a biased method that over-represents more easily sampled population subgroups.

Regarding the term data drift, distinct definitions can be found in the literatures. (Kore et al., 2024) and (Duckworth et al., 2021) define data drift as a "systematic shift in the underlying distribution of input features", where $P_t(X) \neq P_{t+t'}(X)$ for probability distribution P defined at time t. In contrast, (Webb et al., 2016) summarise the term drift such that any of the elements of a joint distribution $P(X,Y)$ might be subject to change over time. Since the joint distribution can be factorized as $P(X,Y) = P(X|Y)P(Y) = P(Y|X)P(X)$, drift occurs if any of $P(X|Y)$, $P(Y|X)$, $P(Y)$ or $P(X)$ change over time. (Quiñonero-Candela et al., 2022) specifies data drift as the circumstance in which the whole joint input-output distribution is non-stationary.

Following the definitions of data drift by (Webb et al., 2016) and (Quiñonero-Candela et al., 2022), we will define data drift as any occurrence of change in the joint distribution over time $P_t(X,Y) \neq P_{t+t'}(X,Y)$.

It is worth mentioning here that data drift is conceptually different from the traditional task of out-of-distribution detection and anomaly detection (Soin et al., 2022), as in (Baugh et al., 2023a). Data drift can manifest as a gradual shift in any of the elements of the joint distribution, whereas individual outliers or anomalies might appear without a data drift. In case of drift detection, the aim is to intervene at model level (*e.g.* retrain, removal from production). On the contrary, if out-of-distribution input is identified, *e.g.* by measuring the difference between the image and its reconstruction (Müller & Kainz, 2022), the assumption is that the model still performs effectively, but was not accurate for that particular input data (Soin et al., 2022).

The most significant reasons for data drift are non-stationary environments (Moreno-Torres et al., 2012). Even if the distribution of the training data matches the data post deployment, it may still be subject to drift over time (Sahiner et al., 2023). In case of non-stationary environments, the training environment differs from the deployment environment due to temporal changes in distribution (Moreno-Torres et al., 2012) thereby violating the stationary assumption underlying ML models (Cieslak & Chawla, 2009).

3.1 Types of Data Drift

Following the terminology by (Moreno-Torres et al., 2012), three different kinds of shift can appear, namely Covariate Shift, Prior Probability Shift and Concept Shift. These shifts do not necessarily have to happen independently from each other, but can happen simultaneously.

When examining dataset shift, the relation between covariates and class labels is highly relevant (Moreno-Torres et al., 2012). Specifically, following our definition of data drift as change in the joint distribution $P_t(X, Y) \neq P_{t+t'}(X, Y)$, and effectively, a change in any of $P(X|Y)$, $P(Y|X)$, $P(Y)$ or $P(X)$, causal and anticausal settings need to be distinguished (Castro et al., 2020) (Schölkopf et al., 2012) in context of the different types of data drifts. Understanding of these two relationships is also key to the understanding and distinguishing the various types of data drifts explained in the following subsections.

- Causal: Estimate $P(Y|X)$ in $X \to Y$ problems, where the class label Y is causally determined by the features X (*e.g.* prediction of labels Y from medical images X) (Moreno-Torres et al., 2012; Castro et al., 2020).
- Anticausal: This is the opposite direction where the goal is to determine $P(X|Y)$ in $Y \to X$ problems, where class label Y causally determines features X (Moreno-Torres et al., 2012; Castro et al., 2020). (Schölkopf et al., 2012) provide examples of class label prediction task from handwritten digits images. The causal structure here is: the person's intention to write a digit (say, 7) causes a motor pattern resulting in the image. Effectively, the class label Y causes X, the image or image features.

(a)   (b)

Figure 5: Graphical causal models illustrating causal relationships between covariates (C), input (X), labels (Y) for (a) Covariate shift: A confounding covariate influences the input, which in turn influences the output, indicating a causal mechanism and (b) Prior Probability Shift: A confounding covariate influences the labels consequently influencing the input, thereby indicating an anticausal mechanism.

In the following subsections, we will elaborate and formalize the three common different kinds of data drifts and their corresponding causal relations.

3.1.1 Covariate Shift

Covariate shift appears only in $X \to Y$ problems, when $P_{TRAIN}(Y|X) = P_{DEPLOYED}(Y|X)$, but $P_{TRAIN}(X) \neq P_{DEPLOYED}(X)$ (Moreno-Torres et al., 2012). Only the covariate distribution is subject to change between the training and the distribution post deployment, and the model $P(Y|X)$ remains unaffected. However, $P_{TRAIN}(X) \neq P_{DEPLOYED}(X)$ should not be mistaken as implying that the rule for the prediction of Y from X does not need to be adapted to the new covariate distribution $P_{DEPLOYED}(X)$. This is reasoned by the fact that predictions based on finite data may favour simple functions that perform well in regions where $P_{TRAIN}(X)$ is high, but not where $P_{DEPLOYED}(X)$ is high (Schölkopf et al., 2012). In the context of causality, by definition, we can remark that covariate shift is associated with causal mechanisms or $X \to Y$ scenarios where the features cause the label, see Figure 5a.

In case of acquisition shift or domain shifts, the measurement system or method of description is subject to change (Quiñonero-Candela et al., 2022). In medical imaging, domain shift is responsible for potentially harmful disparities between development and deployment conditions of medical image analysis techniques. In this context, acquisition shift relates to variations in the likelihood $P_D(X|Z)$ of an image X obtained

from a particular domain D, *e.g.* its appearance, given the unobserved, latent reality Z of a patient's true anatomy (Hognon et al., 2024). Domain or acquisition shift can be understood as a change in the mapping function $X = f(Z)$, where the target variable Y is dependent on the latent, never directly observable variable Z (Quiñonero-Candela et al., 2022). Since a change in the mapping function has an effect on the covariate X, these types of shifts can be seen as subcategories of covariate shift.

In the context of medical imaging, a common cause for covariate shift are different image acquisition devices, *e.g.* multiple manufacturers of scanners or acquisition protocols in clinical use, leading to varying qualities of images. Patient populations subject to change over time also constitute covariate shift (Sahiner et al., 2023), *e.g.* when a new disease appears during a pandemic.

3.1.2 Prior Probability Shift

Prior probability shift occurs only in $Y \to X$ problems or in anticausal settings, when $P_{TRAIN}(Y) \neq P_{DEPLOYED}(Y)$, but the relationship $P_{TRAIN}(X|Y) = P_{DEPLOYED}(X|Y)$ remains (Moreno-Torres et al., 2012), see Figure 5b. The terms label shift and prevalence shift can be used interchangeably for prior probability shift (Castro et al., 2020; Garg et al., 2020).

In case of label shift in diagnostic problems where diseases cause symptoms, the optimal predictor might be subject to change, *e.g.* during a pandemic, the probability of a patient having a disease given their symptoms can increase (Garg et al., 2020). Suppose Y is the target that denotes the probability of a disease with $P(Y = 1) = 0.25$ and $P(Y = 0) = 0.75$. In the event of a pandemic, the disease probability may increase, giving rise to a new probability distribution $P(Y = 1) = 0.5$ and $P(Y = 0) = 0.5$. Although the conditional probability of the disease in the case of a symptom X remains unchanged, *i.e.* $P_{TRAIN}(X|Y) = P_{DEPLOYED}(X|Y)$, the joint distribution $P(X, Y)$ changes due to change in $P(Y)$, causing by definition a data drift induced by prior probability shift.

3.1.3 Concept Shift

Concept shift (Eq. 4) occurs when there is a change in the relationship between X and Y. Following (Moreno-Torres et al., 2012), it can be defined as:

$$P_{TRAIN}(Y|X) \neq P_{DEPLOYED}(Y|X), \text{ but } P_{TRAIN}(X) = P_{DEPLOYED}(X) \text{ in } (X \to Y) \text{ settings}$$
$$P_{TRAIN}(X|Y) \neq P_{DEPLOYED}(X|Y), \text{ but } P_{TRAIN}(Y) = P_{DEPLOYED}(Y) \text{ in } (Y \to X) \text{ settings} \quad (4)$$

Thus, concept shift can occur in both causal and anticausal settings whenever the conditional relation between the cause and effect or the input and target variables changes, see Figure 6. An example of concept shift in causal setting can be seen in the following: After 2020 certain patterns of patchy ground-glass opacity in chest X-rays might not be labelled as bacterial pneumonia anymore, but as COVID-19 pneumonia (Sahiner et al., 2023).

Figure 6: Graphical causal models illustrating causal relationships between confounding covariates (C), input (X), labels (Y) for two distinct cases of concept shift, namely, (a) Concept shift in causal settings: The confounding covariate influences the output, thereby influencing the initial relation between inputs and labels (b) Concept shift in anticausal settings: The confounding covariate influences the input thereby changing the initial anticausal relation.

3.2 Data Drift Assessment and Inherent Challenges

In this subsection, we present several common methods to assess data drift, their current limitations, and the inherent challenges that arise when using these methods.

Data drift assessment can be performed by comparing several commonly used machine learning assessment metrics between the original data domain and the drifted data domain. Performance metrics such as accuracy and segmentation DICE scores are used to determine the performance drop induced by dataset shifts. Uncertainty metrics can be used to determine and identify data drifts, ideally with higher scores signifying higher uncertainties that arise from data drifts:

- *Confidence:* Quantifies the model's uncertainty through the predicted probability of the top class.

- *Entropy:* The sum of the negative log of the prediction probability distribution across all classes.

- *Calibration:* The absolute difference between model's confidence and the prediction empirical accuracies across all classes.

One can measure the domain gap between the original train and test set with several common distributional distance metrics:

- *Fréchet Inception Distance(FID):* Distributional distance between two distinct distributions given their mean and variance.

$$D_F = \|\mu - \mu_{TEST}\|_2^2 + \text{Tr}(\Sigma + \Sigma_{TEST} - 2(\Sigma\Sigma_{TEST})^{\frac{1}{2}}), \tag{5}$$

  where μ represents the mean vector and Σ denotes the covariance matrix of the respective data sets. Tr denotes the trace operator.

- *Maximum Mean Discrepancy(MMD):* Divergence between kernel mean embeddings of the datasets.

$$\text{MMD}^2 = \mathbb{E}[k(\mathbf{x}_{TRAIN}, \mathbf{x}'_{TRAIN})] + \mathbb{E}[k(\mathbf{x}_{TEST}, \mathbf{x}'_{TEST})] - 2\mathbb{E}[k(\mathbf{x}_{TRAIN}, \mathbf{x}_{TEST})], \tag{6}$$

  where $\mathbf{x}_{TRAIN}, \mathbf{x}_{TEST}$ are samples from training and test distributions, and k is a kernel, for example, a Gaussian kernel.

However, there are inherent challenges that hinder the direct applicability of the aforementioned metrics. Performance based methods necessitate ground truth, which might be difficult to obtain in a timely manner or might not be available in general (Kupinski et al., 2002). Uncertainty metrics such as entropy and confidence may also not be reliable as demonstrated by (Ovadia et al., 2019). Direct embedding of data distributions can also be infeasible for real-time drift detections due to the large compute requirements for data of higher dimensions such as higher resolution images. Compared to bias assessment methods, drift assessment methods found in the literature employ a wider variety of other methods and metrics to remedy the potential limitations. We elaborate these methods further in section 5.

3.3 Relevance of Data Drift Detection in Clinical Practice

Data drift can lead to malfunction or performance deterioration of ML models (Sahiner et al., 2023). In the case of classifiers, the negative effect data drift could potentially have on a classifier's performance is caused by a change in the optimal decision boundary (Moreno-Torres et al., 2012). Further, the shifted feature distribution may primarily fall into a region where the model performs poorly (Duckworth et al., 2021).

Therefore, if data drift is detected, a model performance re-evaluation given the current data is necessary, especially in high-stakes scenarios like healthcare (Kore et al., 2024). In case of performance deterioration, appropriate action needs to be taken, such as retraining the model (Duckworth et al., 2021). In the context of healthcare, early detection ensures that reliable medical care can be provided for patients (Kore et al., 2024).

Monitoring the model's performance post-deployment at the output level by comparing the model's output with the ground truth labels is attractive, but is often infeasible due to a lack of ground truth information in ML stratified workflows (Dreiseitl, 2022). Automatic data drift detection can alert operators and allow them to take appropriate actions in terms of model retraining, replacement etc. (Kore et al., 2024). In cases where a drift was detected, but the model's performance did not deteriorate, these insights can be useful in understanding the generalizability of the model to new populations (Kore et al., 2024). Further, it is of high interest to determine the type of changes that occurred between the training and the post-deployment situation (Quiñonero-Candela et al., 2022).

4 Methods for Bias Encoding

This section reviews various approaches that uncover or analyse biases in medical imaging models. The aim is to identify inherent biases that compromise fairness and generalisation for disparate subgroups, and to detect biased models (Seyyed-Kalantari et al., 2020; 2021). The section is organized into: assessing the presence and influence of predefined confounders in machine learning models (Sect. 4.1), assessing unknown confounders via causal inference (Sect. 4.2), and creating datasets for the structured evaluation and comparison of confounder assessment (Sect. 4.3).

4.1 Bias Encoding Assessment

The following methods provide insight into whether bias has been introduced into medical imaging models through confounder variables. We first focus on demographic confounders, such as age, sex, or race. Since clinics can have patients of greatly varying demographics, such confounders can have an immense detrimental impact on clinical practice, especially for minority groups. We then focus on the broader concept of non-demographic confounders, which might affect model performance due to more general forms of shortcut learning.

4.1.1 Demographic Confounders

Detection of Encoded Bias In deep learning architectures, the final layer of a classifier bases its prediction on the features computed by the previous layers of the model. However, how can we determine which information encoded in the features actually leads to the final prediction of the model? To investigate this, we can test whether the information encoded in its features enables the model to solve an unrelated task, such as race prediction. This shows us if additional racial information unrelated to the cancer detection task is present in the features. If the accuracy is high for the race detection task, then this information has to be present in the features. This approach was used by Glocker et al. (2023a), based on the study of Gichoya et al. (2022). They found that a disease classifier backbone trained on a single race has the same race classification results as a backbone without this restriction, which implies that unrelated racial information is present in the features.

However, this does not inform us whether this information is actually *used* for cancer detection, only that it is *present*. We need to employ other methods to detect whether the encoded bias facilitates harmful shortcut learning (see Sect. 2.2.1.)

Influence of Encoded Bias There currently exist two frameworks to predict the influence of encoded biases on the decision making processes in medical imaging: one analysing whether confounders influence the separability of features (Glocker et al., 2023a), the other measuring the correlation between encoding strength and fairness (Brown et al., 2023).

The framework introduced by Glocker et al. (2023a) applies a dimensionality reduction, *e.g.* PCA, to the features of the penultimate layer of a disease classifier. The rationale being that the penultimate layer contains the learned features of the model, while the final layer decides which of the encoded features to use for the task. Given a model trained for disease detection, the strongest separation of samples with and without disease can be found in the first few PCA modes. However, if these also separate other attributes well, then the decision of the model is likely influenced by them. This framework was applied in two follow-

up studies: Piçarra & Glocker (2023) applied this framework to detect biases in generated features in age prediction models based on brain imaging data. They found that some features, which are valuable for age prediction, also contribute to distinguishing between racial and biological sex subgroups. Additionally, Glocker et al. (2023b) used their developed framework (Glocker et al., 2023a) to analyse a recently published chest radiography foundation model (Sellergren et al., 2022) for the presence of biases. An example of how the framework can be applied for this task is illustrated in Example 4.1. Statistically significant differences were observed in ten out of twelve pairwise comparisons across biological sex and race in the foundation model studied, demonstrating racial and sex-related bias. Consequently, this framework allows practitioners, who might have limited insights into foundation model pretraining, to thoroughly assess bias encoding in foundation models applied to downstream tasks (Glocker et al., 2023b).

Example 4.1: Feature Analysis

Principal Component Analysis (PCA) rotates the feature space into orthogonal directions (principal components) ordered by their variance. Projecting data onto the first few components preserves the strongest signals while reducing dimensionality.

Kolmogorov-Smirnov (KS) tests are non-parametric tests that compare the empirical cumulative distributions of two samples and return a p-value indicating whether they stem from the same underlying distribution.

Approach: First, we train the network on radiographs (annotated with disease, sex, race). For every image i store the penultimate layer vector $\mathbf{h}_i$.

Then, we compute the PCA of our features and compute its first four principal components, yielding coordinates $\mathbf{z}_{i1\ldots4}$.

Finally, for each protected attribute and each of the first two PCs, we perform a two-sample Kolmogorov–Smirnov (KS) test.

Example results (significant results in **bold**):

Comparison	p (PC1)	p (PC2)
Disease vs. healthy	1.3×10^{-12}	0.42
Male vs. female	**0.007**	0.52
White vs. Black	0.23	0.18

Conclusion: PC1 cleanly separates disease *and* sex, suggesting the model may exploit sex-specific information (shortcut learning). PC2 appears unrelated to either protected attribute.

The second framework by Brown et al. (2023) assesses the encoding of sensitive attributes, analyses fairness metrics and introduces shortcut testing (ShortT). This provides insights into the correlation between the encoding of the sensitive attribute and fairness metric to investigate how shortcut learning might affect model fairness and performance. The underlying assumption is that the influence of sensitive attributes on the model consists of both biological, potentially causal effects that could improve model performance (graph (a) in Figure 4), and shortcut learning that could be harmful (graph (b) in Figure 4). Even though both scenarios introduce bias, Brown et al. (2023) only refer to shortcut learning when a sensitive attribute is used as confounder, which does not significantly enhance performance, but impacts fairness. To assess the encoding of sensitive attributes such as age in their analysis, they trained a model for disease prediction, froze all weights in the model backbone and then trained a predictor for age using a mean squared error (MSE) regression loss. The performance of the transfer model was measured using the Mean Absolute Error (MAE), which serves as an indicator of the age-related information captured by the final layer of the feature extractor. Lower MAE values correspond to more accurate age predictions, indicating stronger age encoding. To quantify fairness of the model's disease predictions in relation to age, Brown et al. (2023) calculated the separation metric. Separation is defined by fitting two logistic regression models to the binarised model predictions. To this end, the patients were split by the true label: $Y = 1$ (has the condition) and $Y = 0$ (does not). In each split, they fitted a logistic regression that predicts whether the model outputs a positive prediction ($\hat{Y} = 1$ based on age. In the $Y = 1$ group, this tracks how the True Positive Rate (TPR) varies with age, while in the $Y = 0$ group this tracks how the False Positive Rate (FPR) varies with age. Let β_1 be the age coefficient in the $Y = 1$ regression and β_0 the coefficient in the $Y = 0$ regression. Separation is defined

as $Sep = \frac{1}{2}(|\beta_1| + |\beta_0|)$. Values near 0 mean TPR and FPR do not systematically change with age, while larger values mean they do. To assess the degree of age encoding on model fairness, they used a multitask learning model by adding an age prediction head to the base model (disease prediction model) and scaled the gradient updates from the age prediction head. For each value of gradient scaling, they computed the model disease prediction performance, MAE of the age prediction and separation fairness metric. Shortcut learning was indicated by a significant correlation between age encoding and separation fairness metrics (computed via Spearman correlation coefficient). The proposed framework represents a feasible approach for analysing the impact of shortcut learning since the analysis only involves the addition of a demographic prediction head to the base model. Practitioners need to carefully consider which fairness metric to select (besides separation, *e.g.* demographic parity (independence) could be selected), and whether the gradient intervention consistently modifies the encoding of the protected attribute before evaluating its relationship with model fairness (Brown et al., 2023).

4.1.2 Non-Demographic Confounders

The methods proposed below assess the model encoding of non-demographic biases. Such confounders may include any feature in the image that correlates well with a class (see Sect. 2.2.1 for examples). We first give an overview of an important family of non-demographic confounders in biomedical imaging: characteristics introduced during the image acquisition, as introduced by specific CT scanners for example. These works demonstrate that even low-level acquisition cues are perfectly predictable from pixels and can therefore be subject to erroneous shortcut learning. Then we move from discussing specific acquisition-related factors to studies that either create synthetic shortcuts or mask out possible shortcut regions. These methods can be used to detect the presence of any kind of pixel-level confounder.

Shortcuts via Acquisition Parameters Lotter (2024) investigated how acquisition parameters such as view position, field of view, or window size affect race classifiers based on radiographs. They found that changing these parameters strongly influenced model performance, *e.g.* using only lateral view radiographs increases the performance for Asian patients, but decreases the performance for detecting Black patients. They used this insight to mitigate the disease detection performance gap in the baseline dataset between White patients and minorities, by introducing a unique classification threshold for each view position respectively.

In a related study, Badgeley et al. (2019) showed a strong example how radiograph classifiers can largely base their decisions on acquisition parameters rather than pathology. They found that a classifier trained to detect hip fractures using only image data was able to confidently predict both patient-related and acquisition-related metadata. Although the image-only model achieved strong hip fracture classification on the standard data, the performance dropped to pure chance when the fracture vs non-fracture metadata characteristics distributions were equalized. A complementary experiment showed that a classifier only trained on characteristics performed better than the image-only model. The best result were obtained by combining both image data and the characteristics during training.

Shortcut Modification Boland et al. (2024) used Prediction Depth (PD) to detect shortcut learning after adding synthetic shortcuts to the training data. PD measures the example difficulty, *i.e.* the computational effort a trained network needs to make a prediction for a specific input, as the number of layers a model requires to make a final prediction. Boland et al. (2024) linked PD to shortcut learning and the simplicity bias in neural networks, which was originally proposed by Murali et al. (2023), who showed that shortcuts are harmful when they are simpler than the relevant features. To test their method, they trained two binary classification models, one with no shortcuts and the other one with synthesised shortcuts (*e.g.* small red squares, or curved lines added to images), that were perfectly correlated with one class. Both models were evaluated on the same test set, with the shortcuts balanced equally between the two classes. To verify the hypothesis that shortcuts reduce PD, the Welch's t-test was applied to assess whether there was a statistically significant difference in mean PD between the two models. One dataset in their analysis was the CheXpert medical imaging data set (Irvin et al., 2019), where they also introduced synthetic shortcuts to the data. Since the method was only tested on synthetically created shortcuts, its effectiveness on natural shortcuts,

such as site-specific shortcuts in multi-site data, remains to be evaluated. Additionally, the current method has a limitation in that it always requires a dataset without shortcuts as a reference.

In a related work, Sourget et al. (2025) examined whether the model relied on clinically non-relevant parts in radiographs and eye fundus images by systematically masking out irrelevant regions of the image and evaluating disease detection performance. In particular, they trained five different model types: using the unmodified images, masking out the entire region of interest (ROI) bounding box, masking out the exact ROI, masking out everything outside the ROI bounding box, and masking out everything outside the exact ROI. They found that models trained on full images performed better when evaluated on images with the ROI masked than when evaluated on images containing only the ROI. Additionally, models trained only on images with the ROI masked still achieved high classification scores. Both results indicate that the models used features that are not clinically relevant for classification. This result is further exemplified by their experiment in which a trained radiologist was asked to classify radiographs with masked-out ROIs. Unlike the models, the radiologist struggled with this task, which further supports the assumption that the models use characteristics that are not considered relevant by professionals.

Section 4.1 has shown how to detect and quantify the presence and influence of specific, predefined attributes on the decision-making of the model. However, in many cases, the confounding variable is unknown and needs to be characterised as a latent variable. One method for assessing the influence of unknown confounders, *casual inference*, is discussed in the next session.

4.2 Confounding Bias Detection Through Causal Inference

Unlike specifically chosen confounders, such as age or sex, many unknown confounders might be present in the data or in the learned model weights. As demonstrated in Example 4.2, causal inference provides methods to detect such unknown confounders.

> **Example 4.2: Causal Inference**
>
> Assume we have detected a correlation between biological factors $\mathbf{X}$ (*e.g.* age) and a single measure derived from radiographs Y_i (*e.g.* bone age score). How can we rule out a confounding structure $\mathbf{X} \leftarrow \mathbf{Z} \rightarrow \mathbf{Y_i}$ and determine a definite causal relationship between the two? This is the question that causal inference tries to answer. One approach is to use the minimal description length principle: we fit the competing hypotheses and calculate the probability that each assigns to the observed data after averaging over all parameter settings. The hypothesis with the lower description length, *i.e.* the one with the smaller negative log-evidence, is judged the more plausible explanation of the observed correlation.

Wachinger et al. (2019) introduced a method to distinguish between causal and confounded relationships using causal inference. Confounding, with respect to the neuroimaging dataset used in their analysis, refers to imaging site-specific information being implicitly encoded by the model. Notably, the confounders are treated as unknown, latent variables in their method, which is beneficial in complex neuroimaging studies (and also in other medical imaging datasets) where the assumption of causal sufficiency (*i.e.* knowing all confounding variables) is often violated in practice. Their method aims to assess whether X is more likely to cause Y, or if an unobserved random variable Z is the underlying cause of both. Their method leverages the algorithmic Markov condition (AMC), which asserts that if X causes Y, the factorisation of the joint distribution $P(X, Y)$ in the true causal direction will have a lower Kolmogorov complexity than the reverse, anti-causal direction. To approximate Kolmogorov complexity, which is not directly computable, the minimum description length (L) is applied. The factorisation of the causal scenario $P(X, Y)_{ca} = P(Y \mid X)P(X \mid Z)P(Z)$ is represented by a linear regression model, whereas the factorisation of the confounded scenario $P(X, Y)_{co} = P(Y \mid Z)P(X \mid Z)P(Z)$ is estimated by probabilistic PCA. To compare the causal with the confounded model $\Delta(X, Y) = L_{co}(X, Y) - L_{ca}(X, Y)$ is computed. If the causal model provides a better fit to the data than the confounded model then $\Delta(X, Y) > 0$. It has to be noted that inferring causality from observational data is difficult because the true causal effects and their magnitudes are unknown, making quantitative evaluation impossible.

While the previous methods have allowed us to gain some insight into the influence certain data attributes have on a model, we currently lack evidence of how well these methods perform under specific conditions, systematic ways to evaluate the effect of different dataset characteristics, and a level playing field on which to compare bias assessment algorithms. For this purpose, dataset creation methods have been developed.

4.3 Representative Datasets For Bias Assessment

The following methods focus on creating datasets to mitigate and study bias. Either by constructing datasets with controlled bias components for evaluating bias mitigation, or removing bias directly from the dataset, so no further bias mitigation is necessary.

To objectively analyse the impact of biases on medical imaging models without the limitations of real-world datasets (*e.g.* unknown confounding factors), Stanley et al. (2023) proposed SimBA, a versatile framework for generating synthetic neuroimaging data with controlled simulation of disease, bias, and subject effects. Synthetic images were generated by applying non-linear diffeomorphic transformations to a template image I_T that represents the average brain morphology. Non-linear transformations for disease and bias were spatially localised deformations to I_T whereas the subject morphology was generated through a global non-linear transformation. These effects and deformations were derived from PCA-based generative models of these non-linear deformations. Each effect represented a specific degree of morphological variation within the typical range of inter-subject human brain anatomy. This method allows to generate synthetic datasets with controlled bias effects. However, it has to be noted that expert knowledge is required to define the brain regions for the localised deformation for the disease and bias effects. Furthermore, it needs to be highlighted that the introduced biases were not designed to replicate any particular real-world sociodemographic sub-population, as the imaging features that introduce bias within these groups are often complex, interrelated and/or unknown. Instead, the simulated biases create hypothetical subgroups within a dataset that exhibit specific confounding features, which may lead to shortcut learning in medical imaging ML models. However, the synthetically biased datasets provide an opportunity to test bias mitigation strategies.

Stanley et al. (2024b) extended their research on the SimBA framework (Stanley et al., 2023) by using this tool to study bias manifestations and the effectiveness of bias mitigation techniques. They generated counterfactual neuroimaging datasets with three bias scenarios (*i.e.* No Bias, Near Bias, Far Bias with Near and Far indicating the proximity to the voxels representing disease). By incorporating unequal proportions of biased brain images for the disease class and non-disease class (70% vs. 30% containing bias) they incorporated the possibility of the model to use bias as shortcut for predicting the disease. At the same time they ensured that subject and disease effects were similar for each bias group (preventing unwanted additional source of bias) enabling a controlled evaluation of bias. Stanley et al. (2024b) then used these synthetically generated images to assess the efficiency of various bias mitigation strategies (reweighing, unlearning, group models). The SimBA framework represents an interesting approach to test models for bias encoding, but the bias scenarios that can be generated by this framework are limited to scenarios in which biases are represented by localised spatial deformations, or are related to intensity-based simulated artifacts. Real-world medical imaging data can be more complex and inherently contain numerous confounding and interacting biases.

Apart from these synthetically generated biased/unbiased datasets, Glocker et al. (2023a) used strategic resampling with replacement to create balanced test sets that represent the population of interest. The goal was not replicating dataset bias in the test set (due to random splitting of the original dataset) and to allow an unbiased estimation of performance on different race subgroups. Specifically, they used resampling with replacement to create race balanced test sets while controlling for age differences and disease prevalence for each racial group.

5 Methods for Data Drift Detection

This section provides an overview of methods developed for data drift detection in a general setting for prevalence drift (Sect. 5.1) and covariate drift (Sect. 5.2). The following section presents a multitude of approaches in more detail, focussing on the application in the medical imaging domain (Sect. 5.3). We follow the common categorisation into classifier-based, feature-based, and metadata-based approaches.

5.1 Prevalence Drift Detection

Roschewitz et al. (2023) introduced Unsupervised Prediction Alignment (UPA), which was originally designed to recover the desired sensitivity/specificity trade-off in the case of acquisition shift. UPA can also be applied to detect prevalence shift. This involves using linear piecewise cumulative distribution matching to align the prediction distribution from the unseen dataset with a reference distribution of fixed prevalence. In the case of prevalence shift detection, the mean absolute difference between the original (shifted) and aligned predictions is calculated. When there is no prevalence shift present in the data, the difference should be 0. A limitation of this method is that it only detects shifts in prevalence, reducing its clinical practicality as it would need to be used alongside other drift detection techniques.

5.2 Covariate Drift Detection

5.2.1 Dimensionality Reduction

Rabanser et al. (2019) base their analysis of shift detection between imaging source (training) and target data (artificially shifted data) on common dimensionality reduction methods combined with two-sample tests. Dimensionality reduction methods try to compress the numerical representation of extracted features, by transforming the feature vector into a smaller one without losing important information (*i.e.* preserving structure between feature vectors of different samples). This transformation can either be learned (*e.g.* Auto-Encoders, cf. Example 5.1) or constructed analytically (*e.g.* PCA, cf. Example 4.1). To compare the differences between the source and shifted dataset after reducing their dimensions, the authors used several statistical methods, especially the Maximum Mean Discrepancy (MMD), cf. Equation 6, to compare the multivariate distributions and the Kolmogorov-Smirnov (KS) test for individual dimensions separately.

Rabanser et al. (2019) used the MNIST and CIFAR-10 datasets for their analysis and simulate shifts affecting both covariate and label proportions. Their compared methods include PCA, sparse random projections, trained and untrained Auto-Encoders (tAE, uAE), label classifier, and domain classifier. They find that the Softmax outputs from the trained label classifier combined with multiple univariate KS testing yields the best performance in shift detection, followed by multivariate-testing of an untrained Auto-Encoder embedding.

It has to be highlighted that the number of target (shifted) data samples has a substantial influence on the accuracy of the shift detection. This has to be taken into consideration when applying the shift detection methods in practice. Consequently, selecting an appropriate rolling window time frame is essential to have a sufficient amount of data samples to compare with the reference (training) data. Since the shift detection based on Softmax outputs combined with KS testing can be easily added on top of an already trained classifier, this method constitutes a feasible practical solution.

Example 5.1: Auto-Encoder

Auto-Encoders are a common and simple network architecture that draws inspiration from sparse coding and works in an unsupervised manner. The architecture consists of two parts, the Encoder and the Decoder. Both a trained in tandem while during inference only one of the two, depending on the application, is used. The key aspect is a information bottleneck between Encoder and Decoder. Specifically, the Encoder transforms the input over several non-linear layers into a lower dimensional representation (the bottleneck), while the Decoder, acting as regularisation, has to be able to reconstruct the original input using only the compressed representation. Hence, the objective function is minimizing the reconstruction error between input and output, typically measured as the MSE.

Variational Auto-Encoders are a probabilistic extension of the classical Auto-Encoder. Specifically, their bottleneck does not represent a deterministic lower dimensional feature space, but defines independent distributions for each compressed dimension, *e.g.* mean and variance of an assumed Gaussian distribution. These latent distributions allow the generation of new samples (images) that appear close to the training sample distribution, *e.g.* by drawing from every Gaussian in the bottleneck.

5.2.2 Uncertainty Estimation

Investigating the metrics discussed in Sect. 3.2, Ovadia et al. (2019) use approaches of uncertainty estimation for identifying data drift in image data. Their findings suggest that entropy scores and prediction confidence are ineffective when tested on out-of-distribution (OOD) data (based on a class excluded from the training set in the MNIST dataset). Most calibrated models exhibit low entropy and high confidence in their study, meaning they were confidently incorrect when predicting entirely OOD data. Consequently, changes in these two metrics do not provide a reliable indication of data drift leading to increased uncertainty, as measured by entropy scores and prediction confidence. Concerning the Expected Calibration Error (ECE) they found that ECE increased as the shift intensity grew. However, since ECE depends on ground truth labels, using this measure to detect drift is not practical for automated drift detection in clinical settings.

5.2.3 Image Segmentation

To predict segmentation performance in the absence of ground truth labels, Valindria et al. (2017) propose reverse classification accuracy (RCA). Specifically, a classifier is trained on a single image with its predicted segmentation (where the segmentation prediction of this single image is derived from the original segmentation model) serving as pseudo ground truth (GT). The method is built on the assumption that if the segmentation quality for a new image is high, then the RCA classifier trained on the predicted segmentation used as pseudo GT will perform well at least on some of the images in the reference database. Similarly, if the segmentation quality is poor, the classifier is likely to perform poorly on the reference images. The Reverse classifiers that are used in the study are Atlas forests (Zikic et al., 2014), the CNN model DeepMedic (Kamnitsas et al., 2017b) with a decreased amount of filters and consequently parameters to reduce overfitting to the single image input, and Atlas-based label propagation (Bai et al., 2013). It is important to note that the reference database used for evaluation can be the same as, or different from, the training database employed for training, cross-validation, and fine-tuning the original segmentation method. For measuring the segmentation accuracy the maximum Dice score coefficient value that is found across all reference images is used. They found that Atlas Forests and in particular, Single-Atlas label propagation yield accurate predictions (in terms of mean absolute error and correlation between predicted and true dice score coefficient) for different segmentation methods.

5.3 Drift Detection in the Medical Domain

Even though domain adaptation, which becomes relevant in case of dataset shift (domain shift), has gained significant attention over the last years (Guan & Liu, 2021), the methods on mere detection of data drift in the medical imaging context are still limited (Sahiner et al., 2023). This section will provide an overview of successfully applied drift detection methods for medical imaging workflows.

5.3.1 Classifier Based

Kore et al. (2024) applied dimensionality reduction using a trained Auto-Encoder (tAE) alongside Softmax outputs from a model trained on the source data, drawing parallels to the work of Rabanser et al. (2019). They employed their approach to detect data drift in chest X-ray images. The trained Auto-Encoder is a TorchXRayVision Auto-Encoder (Cohen et al., 2022) and the trained classifier is a TorchXRayVision model. They applied the MMD statistical test on the resulting dimensionally reduced embeddings to identify statistical differences between the source and target data. The shift detection methods were tested on temporal imaging data, which initially constituted natural shifts (such as the introduction of COVID-19 in 2020, which caused a prevalence shift), and synthetically shifted data investigating specific population shifts. The shift factors studied were institution, sex, patient age, patient class, and ICU admission status. The authors found a correlation between the sensitivity of drift detection and the magnitude of the synthetic drift, with the tAE+trained classifier combination proving more sensitive than tAE alone, and the trained classifier being nearly as sensitive as the combined method.

Koch et al. (2024) tackled the challenge of detecting clinically significant distribution shifts in retinal imaging data gathered during diabetic retinopathy screenings from multiple hospitals, each with diverse demographic populations. They employed a domain classifier to distinguish between the source and shifted datasets.

They also performed MMD tests, where the kernel was parametrised by a neural network, which was trained separately on the source and shifted training sets. Additionally, they analysed the softmax prediction outputs of a classifier trained to predict the C classes from the source dataset, using multiple univariate Kolmogorov-Smirnov tests. Similar to the approach taken by Kore et al. (2024), they simulated subgroup shifts based on patient characteristics such as sex, ethnicity, image quality, and the presence of co-morbidities. For example, a shift in patient sex was simulated by including only images from female patients in the target distribution. Their experiments demonstrated that classifier-based tests consistently and significantly outperformed the other methods. However, crucial covariates that define relevant subgroup characteristics are often unmeasured or unidentified. Therefore by only controlling for a fraction of possible covariates, the shift might not be originating from the shifted feature, but from an altered composition of unobserved covariates.

5.3.2 Feature Based

The work of Stacke et al. (2020) focused on quantifying the magnitude of domain shift by measuring shift in the learnt representation space of Histopathology imaging data. Under the assumption that in a well-trained model a convolutional layer will focus on image features that are relevant to the specific task and irrelevant features are discarded, Stacke et al. (2020) developed a metric (the representation shift metric R_l, which is defined for each layer l) that analyses the filter activations in each layer of a given CNN model. Even if the differences between the two domains appear minor in the image space, variations in training data statistics can lead to significant discrepancies in the internal model representations. First, all samples from the source and target dataset are passed through the model and for each layer l and filter k the feature maps $\varphi_{l,k}$ are averaged over the image dimensions h and w:

$$c_{lk}(x) = \frac{1}{hw} \sum_{i,j}^{h,w} \varphi_{l,k}(x)_{i,j} \tag{7}$$

Next, the representation shift R_l is derived by calculating the discrepancy between the distributions of c_{lk} between the source and target dataset and then taking the average over all filters, which results in one R_l per layer. In their study Stacke et al. (2020) evaluated three discrepancy metrics: Wasserstein distance, Kullback-Leibler divergence, and Kolmogorov-Smirnov statistic. If the data samples from the source and the target domains are statistically similar in the network's representation space, meaning a small representation shift R_l, then the target domain should be close to the source domain. Since the metric does not rely on annotated data, it can be used as a straightforward initial test to assess whether new data (*e.g.* histopathology images from a different scanner) is properly handled by an already trained model, *e.g.* whether the learned feature representation applies to the new data.

To increase quality and quantity of medical data curation, Guo et al. (2023) propose MedShift as an automatic pipeline to combine datasets across different institutions. The approach assumes an available internal dataset which is treated as baseline for evaluation of *shiftness* in external datasets. They demonstrate their method on two domains, namely musculoskeletal radiographs (MURA) with Stanford MURA (Rajpurkar et al., 2017) as external dataset, and chest X-rays with CheXpert (Irvin et al., 2019) and MIMIC (Johnson et al., 2019) as external datasets. Variational Auto-Encoders (VAE) are trained separately on each class of the internal dataset, thereby, learning a distributional representation which is queried and fed into a binary discriminator assessing whether the reconstructed query is part of the class distribution. Then the anomaly score is the sum of the reconstruction error of the VAE and the discriminator's prediction, with high scores indicating shift data. On the external dataset, the anomaly score is then calculated for each class and serves as the metric to construct an unsupervised class-wise clustering. Finally, the *shiftness* is quantified by evaluating a multi-class classifier trained on the internal dataset on the external dataset, by successively removing clusters with the highest anomaly score in each class, and monitoring the classifier's performance increase.

The proposed method is efficient to detect variability between datasets when they exhibit the same classes and could potentially be used to assess if a given dataset is similar to the training set used for model training. In their analysis, Guo et al. (2023) found that higher anomaly groups are originating from variations in positioning, noise and image quality. Therefore, further investigation is needed to determine the specific types of shifts to which this method is sensitive.

5.3.3 Metadata Based

Additionally to image features, Merkow et al. (2023) also integrated DICOM metadata (*e.g.* patient demographics, image formation metadata, image storage information) and predicted probabilities into an aggregated metric to detect temporal data drift in X-ray datasets using Rolling Detection Windows. To encode image appearance-based features and derive the latent space representation, they use a Variational Auto-Encoder (VAE), cf. Example 5.1. The statistical significance of the detected drift in continuous and categorical features is verified with Kolmogorov-Smirnov and Chi-Squared tests respectively. Merkow et al. (2023) simulated two drift scenarios: (1) performance degradation – randomly populating the stream of original data with hard data by only focusing on samples where the classifier exhibits low confidence for individual labels – and (2) clinical workflow failure – introducing lateral view images which the model was not trained on; adding paediatric data that typical ML models are not authorised to report on. They could show that statistical significant variation in model inputs and outputs can be useful indicators of potential declines in model performance.

6 Discussion

Table 1: Comparison of Bias Encoding Assessment, Data Drift Detection, Harmfulness Estimation, and Application in Medical Imaging Studies.

Approach	Bias Assessment			Data Drift Detection					Harmfulness Evaluation		Application	
	Demographic Confounder	Non-Demographic Confounder	Synthetic Bias Datasets	Drift Detection	Prevalence Drift	Shift Detection	Synthetic Drift	Natural Drift	Drift Severity	Segmentation Accuracy	RGB Image Data	Medical Imaging Data
Glocker et al. (2023a)	✓		✓								✓	✓
Glocker et al. (2023b)	✓										✓	✓
Piçarra & Glocker (2023)	✓										✓	✓
Brown et al. (2023)	✓										✓	✓
Boland et al. (2024)		✓									✓	✓
Wachinger et al. (2019)	✓	✓									✓	✓
Stanley et al. (2023)			✓								✓	✓
Stanley et al. (2024b)			✓								✓	✓
Rabanser et al. (2019)				✓			✓		✓		✓	
Ovadia et al. (2019)				✓			✓				✓	
Kore et al. (2024)				✓			✓	✓			✓	✓
Koch et al. (2024)				✓			✓				✓	✓
Merkow et al. (2023)				✓			✓				✓	✓
Stacke et al. (2020)				✓			✓				✓	✓
Roschewitz et al. (2023)				✓	✓		✓				✓	✓
Guo et al. (2023)						✓	✓				✓	✓
Valindria et al. (2017)										✓	✓	✓

In Sect. 4 and 5 we discuss methods to ensure reliable ML model deployment and maintain consistent prediction performance over time in clinical settings. Most of the methods presented have been tested on medical imaging data, while some, particularly those in Sect. 5.2 (drift detection), still need to be evaluated for this domain. To ease comparison between the discussed approaches we have summarised their problem domain in Table 1.

The bias encoding assessment methods outlined in Sect. 4.1 can help practitioners gain transparency regarding bias encoding in pre-trained medical imaging models and to derive tailored bias mitigation strategies. Beyond assessing bias through output prediction disparities across sensitive subgroups (sex, race, age), examining the inner workings of bias encoding offers insights into how sensitive attributes are inter-related with

each other and related with the primary task (disease detection). As Brown et al. (2023) and Glocker et al. (2023a) have demonstrated, encoding of sensitive attributes does not necessarily mean that those features are used for the primary task prediction. If bias is present, the impact of these sensitive attributes on model performance should be analysed (*e.g.* with the method proposed by Brown et al. (2023)) to distinguish between scenarios (a) and (b) as shown in Figure 4.

Further research is required to determine whether the findings of Glocker et al. (2023b) on bias encoding in chest radiography foundation models also apply to other foundation models. Given the high popularity of foundation models in the medical field (Azad et al., 2023) and the foundation models' use as a basis for other downstream task applications represents a key concern since any inherent biases of the foundation models might be inherited by all models that are fine-tuned on them (Bommasani et al., 2021). Therefore, it is crucial to tackle and alleviate biases in foundation models to guarantee fairness, inclusiveness, and ethical development within the medical domain (Azad et al., 2023).

Beyond demographic factors, works based on changing specific parameters (Lotter, 2024), or image modification (Boland et al., 2024; Sourget et al., 2025) demonstrated the strong influence of non-demographic biases on model decisions. While some of the proposed methods can be used to analyse the influence of specifically selected attributes on model outcomes, there exists no widely adopted framework to detect general forms of shortcut learning in medical imaging to our knowledge. However, extending and improving synthetic bias generation frameworks such as SimBA (Stanley et al., 2023), so that they can accurately represent most real-world biases in the medical domain, might be a promising step in this direction.

Determining the root causes of performance disparities remains challenging and will require future research. The presence of multiple potential sources of bias, including selection bias, annotation bias, and algorithmic bias – both demographic and non-demographic – makes it challenging to pinpoint the exact factors contributing to the disparities. Additionally, the interconnections between these biases complicate causal bias determination.

In addition to efforts aimed at mitigating bias in models trained on medical imaging data (Dinsdale et al., 2021; Correa et al., 2021; Yang et al., 2024b), it is crucial to collect a representative dataset to prevent the model from inheriting dataset bias. Attention should also be given to the labelling process, with procedures in place to resolve multi-annotator label disagreements, ensuring unbiased labels.

When developing models, there is an inherent trade-off between tailoring a model to the specific deployment population – while risking bias from the under- or overrepresentation of certain subgroups – and creating a model based on a more representative dataset for the broader population (using *e.g.* reweighing strategies). The former approach may not generalise well to hospitals in other countries with different patient demographics, while the latter may lack the specificity needed for the deployment population, requiring fine-tuning for optimal performance.

Most of the drift detection methods discussed in Section 5.2 were evaluated on simulated data drifts. Thus, future research is necessary to assess these methods on real data drifts. However, this poses a challenge, as, given we are mostly relying on temporal imaging data from a single source, it is inherently difficult to determine when a true statistically significant shift has occurred, which is essential for validating the effectiveness of these methods.

For implementing drift detection methods, it is crucial to set the intervals at which drift detection will be applied, thereby determining the appropriate number of images needed for the target dataset. Kore et al. (2024) found that increasing the number of images in the target set improves sensitivity. However, this may not be feasible for smaller institutions or ML applications that handle relatively few cases, such as rare diseases. Thus, institutions may need to balance the frequency of drift detection with its sensitivity.

When a statistically significant data drift was detected and performance deterioration was estimated, expert labelling is necessary to annotate the data collected between the original model deployment and the drift detection timepoint. This step is crucial to confirm whether there was an actual decline in performance. Then retraining and re-validation of the model is necessary.

An intriguing area of study arises when drift is detected without corresponding performance deterioration. In such cases, analysing which covariates have changed (*e.g.* patient demographics, scanner type) through exploratory analysis can provide insights into which populations the model remains generalizable to. However, this analysis must be approached with caution, as, even if generalizability to certain populations is observed, there is no guarantee that the model is generalizable to populations with similar distributions, since unknown confounding factors may still be present.

In this work, we primarily focus on methods for *detecting* bias and data drifts, leaving the discussion of automated mitigation strategies for future exploration. Alternatives to re-labelling, re-training, and re-evaluation are not covered in depth. Nevertheless, we highlight two promising directions that merit further exploration in the literature: (a) domain adaptation techniques (see, e.g., (Kamnitsas et al., 2017a; Ouyang et al., 2019; 2022b;a; Guan & Liu, 2021; Chen et al., 2019)), which modify inputs to align them with a target distribution where a trained model remains effective, and (b) out-of-distribution detection approaches (see, e.g., (Yang et al., 2024a; Zimmerer et al., 2022; Tan et al., 2021; Schlüter et al., 2022; Naval Marimont et al., 2024; Baugh et al., 2023b; P. Müller et al., 2023; Baugh et al., 2022)), often coupled with biased model selection, where models tailored to specific populations are chosen based on explicit or implicit patient class parameters.

The first avenue has already demonstrated encouraging results in transferring tasks across modalities (Ouyang et al., 2022b), while the second offers a practical pathway for production deployment, though it requires careful validation for each sub-population. Readers interested in mitigation strategies beyond detection may find these works particularly valuable as starting points.

7 Conclusion

The safe integration of machine learning into clinical practice requires robust systems that are reliable and effective. The ideal of total fairness remains elusive, as group-level statistical parity can conflict with individual-level accuracy and clinically relevant correlations. Therefore, the practical goal is to make model biases tractable and interpretable. In this survey, we present a unified framework for addressing two critical threats to this reliability: unexamined bias encoded during development and performance degradation from data drift post-deployment. Our work provides a critical overview of the state-of-the-art methods needed to identify these challenges, even when ground truth is unavailable. This pursuit of transparency is not merely a technical exercise but an ethical and regulatory imperative. Emerging regulations, such as the EU AI Act (European Council, 2023) and California's AI legislation (California State Legislature, 2023b;a), mandate a shift from static validation to continuous life-cycle governance. These frameworks demand the very tractability this survey champions: the ability to monitor performance, understand potential discrimination risks, and make informed decisions to ensure patient safety and build clinical trust (European Commission, 2021). The methods we review are foundational to meeting these requirements. By unifying the concepts of bias assessment and drift detection, our survey provides an essential roadmap for the medical AI community. It equips researchers and clinicians with the integrated perspective needed to move beyond the pursuit of perfect fairness and toward the development of resilient AI systems. The goal is to create tools where biases are not just hidden liabilities but are identified, understood, and managed.

References

Mujaheed Abdullahi, Hitham Alhussian, Norshakirah Aziz, Said Jadid Abdulkadir, Yahia Baashar, Abdussalam Ahmed Alashhab, and Afroza Afrin. A systematic literature review of concept drift mitigation in time-series applications. *IEEE Access*, 13:119380–119410, 2025.

Anissa Alloula, Charles Jones, Ben Glocker, and Bartlomiej Papiez. Subgroups matter for robust bias mitigation. In *Forty-second International Conference on Machine Learning*, 2025. URL https://openreview.net/forum?id=P0RkH1RT5z.

Philippe Autier, Magali Boniol, Alice Koechlin, Cécile Pizot, and Mathieu Boniol. Effectiveness of and overdiagnosis from mammography screening in the netherlands: population based study. *bmj*, 359, 2017.

Bobby Azad, Reza Azad, Sania Eskandari, Afshin Bozorgpour, Amirhossein Kazerouni, Islem Rekik, and Dorit Merhof. Foundational models in medical imaging: A comprehensive survey and future vision. *arXiv preprint arXiv:2310.18689*, 2023.

Marcus A. Badgeley, John R. Zech, Luke Oakden-Rayner, Benjamin S. Glicksberg, Manway Liu, William Gale, Michael V. McConnell, Bethany Percha, Thomas M. Snyder, and Joel T. Dudley. Deep learning predicts hip fracture using confounding patient and healthcare variables. *npj Digital Medicine*, 2(1):31, April 2019. ISSN 2398-6352. doi: 10.1038/s41746-019-0105-1. URL https://doi.org/10.1038/s41746-019-0105-1.

Wenjia Bai, Wenzhe Shi, Declan P O'regan, Tong Tong, Haiyan Wang, Shahnaz Jamil-Copley, Nicholas S Peters, and Daniel Rueckert. A probabilistic patch-based label fusion model for multi-atlas segmentation with registration refinement: application to cardiac mr images. *IEEE transactions on medical imaging*, 32 (7):1302–1315, 2013.

Imon Banerjee, Kamanasish Bhattacharjee, John L Burns, Hari Trivedi, Saptarshi Purkayastha, Laleh Seyyed-Kalantari, Bhavik N Patel, Rakesh Shiradkar, and Judy Gichoya. "shortcuts" causing bias in radiology artificial intelligence: causes, evaluation and mitigation. *Journal of the American College of Radiology*, 2023.

Solon Barocas, Moritz Hardt, and Arvind Narayanan. *Fairness and machine learning: Limitations and opportunities*. MIT press, 2023.

Matthew Baugh, Jeremy Tan, Athanasios Vlontzos, Johanna P Müller, and Bernhard Kainz. nnood: A framework for benchmarking self-supervised anomaly localisation methods. In *International Workshop on Uncertainty for Safe Utilization of Machine Learning in Medical Imaging*, pp. 103–112. Springer, 2022.

Matthew Baugh, James Batten, Johanna P Müller, and Bernhard Kainz. Zero-shot anomaly detection with pre-trained segmentation models. *arXiv preprint arXiv:2306.09269*, 2023a.

Matthew Baugh, Jeremy Tan, Johanna P Müller, Mischa Dombrowski, James Batten, and Bernhard Kainz. Many tasks make light work: Learning to localise medical anomalies from multiple synthetic tasks. In *International Conference on Medical Image Computing and Computer-Assisted Intervention*, pp. 162–172. Springer, 2023b.

Mélanie Bernhardt, Charles Jones, and Ben Glocker. Potential sources of dataset bias complicate investigation of underdiagnosis by machine learning algorithms. *Nature Medicine*, 28(6):1157–1158, 2022.

Christopher Boland, Keith A Goatman, Sotirios A Tsaftaris, and Sonia Dahdouh. There are no shortcuts to anywhere worth going: Identifying shortcuts in deep learning models for medical image analysis. In *Medical Imaging with Deep Learning*, 2024.

Rishi Bommasani, Drew A Hudson, Ehsan Adeli, Russ Altman, Simran Arora, Sydney von Arx, Michael S Bernstein, Jeannette Bohg, Antoine Bosselut, Emma Brunskill, et al. On the opportunities and risks of foundation models. *arXiv preprint arXiv:2108.07258*, 2021.

Alexander Brown, Nenad Tomasev, Jan Freyberg, Yuan Liu, Alan Karthikesalingam, and Jessica Schrouff. Detecting shortcut learning for fair medical ai using shortcut testing. *Nature communications*, 14(1):4314, 2023.

Danielle L Brown. Bias in image analysis and its solution: unbiased stereology. *J Toxicol Pathol*, 30(3): 183–191, 2017.

California State Legislature. California assembly bill no. 2013, 2023a. URL https://leginfo.legislatur e.ca.gov/faces/billNavClient.xhtml?bill_id=202320240AB2013. Accessed: September 22, 2024.

California State Legislature. California senate bill no. 1047, 2023b. URL https://leginfo.legislature. ca.gov/faces/billNavClient.xhtml?bill_id=202320240SB1047. Accessed: September 22, 2024.

Alessandro Castelnovo, Riccardo Crupi, Greta Greco, Daniele Regoli, Ilaria Giuseppina Penco, and Andrea Claudio Cosentini. A clarification of the nuances in the fairness metrics landscape. *Scientific Reports*, 12(1):4209, 2022.

Daniel C Castro, Ian Walker, and Ben Glocker. Causality matters in medical imaging. *Nature Communications*, 11(1):3673, 2020.

Danton S Char, Nigam H Shah, and David Magnus. Implementing machine learning in health care—addressing ethical challenges. *The New England journal of medicine*, 378(11):981, 2018.

Cheng Chen, Qi Dou, Hao Chen, Jing Qin, and Pheng-Ann Heng. Synergistic image and feature adaptation: Towards cross-modality domain adaptation for medical image segmentation. In *Proceedings of the AAAI conference on artificial intelligence*, volume 33, pp. 865–872, 2019.

Jiaee Cheong, Sinan Kalkan, and Hatice Gunes. Causal structure learning of bias for fair affect recognition. In *Proceedings of the IEEE/CVF Winter Conference on Applications of Computer Vision*, pp. 340–349, 2023.

Alexandra Chouldechova. Fair prediction with disparate impact: A study of bias in recidivism prediction instruments. *Big data*, 5(2):153–163, 2017.

David A Cieslak and Nitesh V Chawla. A framework for monitoring classifiers' performance: when and why failure occurs? *Knowledge and Information Systems*, 18(1):83–108, 2009.

Joseph Paul Cohen, Joseph D Viviano, Paul Bertin, Paul Morrison, Parsa Torabian, Matteo Guarrera, Matthew P Lungren, Akshay Chaudhari, Rupert Brooks, Mohammad Hashir, et al. Torchxrayvision: A library of chest x-ray datasets and models. In *International Conference on Medical Imaging with Deep Learning*, pp. 231–249. PMLR, 2022.

Ramon Correa, Jiwoong Jason Jeong, Bhavik Patel, Hari Trivedi, Judy W Gichoya, and Imon Banerjee. Two-step adversarial debiasing with partial learning–medical image case-studies. *arXiv preprint arXiv:2111.08711*, 2021.

James L Cross, Michael A Choma, and John A Onofrey. Bias in medical ai: Implications for clinical decision-making. *PLOS Digital Health*, 3(11):e0000651, 2024.

Carolynn M DeBenedectis, Lucy B Spalluto, Lisa Americo, Casey Bishop, Asim Mian, David Sarkany, Nolan J Kagetsu, and Priscilla J Slanetz. Health care disparities in radiology—a review of the current literature. *Journal of the American College of Radiology*, 19(1):101–111, 2022.

Sepehr Dehdashtian, Ruozhen He, Yi Li, Guha Balakrishnan, Nuno Vasconcelos, Vicente Ordonez, and Vishnu Naresh Boddeti. Fairness and bias mitigation in computer vision: A survey. *arXiv preprint arXiv:2408.02464*, 2024.

Neofytos Dimitriou, Ognjen Arandjelović, and Peter D Caie. Deep learning for whole slide image analysis: an overview. *Frontiers in medicine*, 6:264, 2019.

Nicola K Dinsdale, Mark Jenkinson, and Ana IL Namburete. Deep learning-based unlearning of dataset bias for mri harmonisation and confound removal. *NeuroImage*, 228:117689, 2021.

Stephan Dreiseitl. A comparison of covariate shift detection methods on medical datasets. In *International Conference on Computer Aided Systems Theory*, pp. 487–495. Springer, 2022.

Karen Drukker, Weijie Chen, Judy Gichoya, Nicholas Gruszauskas, Jayashree Kalpathy-Cramer, Sanmi Koyejo, Kyle Myers, Rui C Sá, Berkman Sahiner, Heather Whitney, Zi Zhang, and Maryellen Giger. Toward fairness in artificial intelligence for medical image analysis: identification and mitigation of potential biases in the roadmap from data collection to model deployment. *J. Med. Imaging (Bellingham)*, 10(6): 061104, 2023.

Christopher Duckworth, Francis P Chmiel, Dan K Burns, Zlatko D Zlatev, Neil M White, Thomas WV Daniels, Michael Kiuber, and Michael J Boniface. Using explainable machine learning to characterise data drift and detect emergent health risks for emergency department admissions during covid-19. *Scientific reports*, 11(1):23017, 2021.

Cynthia Dwork, Moritz Hardt, Toniann Pitassi, Omer Reingold, and Richard Zemel. Fairness through awareness. In *Proceedings of the 3rd innovations in theoretical computer science conference*, pp. 214–226, 2012.

European Commission. Proposal for a regulation of the european parliament and of the council laying down harmonised rules on artificial intelligence (artificial intelligence act) and amending certain union legislative acts, 2021. URL https://eur-lex.europa.eu/legal-content/EN/TXT/?uri=celex:52021PC0206. Accessed: 2024-09-22.

European Council. Artificial intelligence act: Council and parliament strike a deal on the first worldwide rules for ai, 2023. URL https://www.consilium.europa.eu/de/press/press-releases/2023/12/09/artificial-intelligence-act-council-and-parliament-strike-a-deal-on-the-first-worldwide-rules-for-ai/. Accessed: 2024-09-22.

João Gama, Indrundefined Žliobaitundefined, Albert Bifet, Mykola Pechenizkiy, and Abdelhamid Bouchachia. A survey on concept drift adaptation. *ACM Comput. Surv.*, 46(4), 2014. ISSN 0360-0300. doi: 10.1145/2523813.

Jianhui Gao, Benson Chou, Zachary R McCaw, Hilary Thurston, Paul Varghese, Chuan Hong, and Jessica Gronsbell. What is fair? defining fairness in machine learning for health. *arXiv preprint arXiv:2406.09307*, 2024.

Saurabh Garg, Yifan Wu, Sivaraman Balakrishnan, and Zachary Lipton. A unified view of label shift estimation. *Advances in Neural Information Processing Systems*, 33:3290–3300, 2020.

Milena A Gianfrancesco, Suzanne Tamang, Jinoos Yazdany, and Gabriela Schmajuk. Potential biases in machine learning algorithms using electronic health record data. *JAMA internal medicine*, 178(11):1544–1547, 2018.

Judy Wawira Gichoya, Imon Banerjee, Ananth Reddy Bhimireddy, John L Burns, Leo Anthony Celi, Li-Ching Chen, Ramon Correa, Natalie Dullerud, Marzyeh Ghassemi, Shih-Cheng Huang, et al. Ai recognition of patient race in medical imaging: a modelling study. *The Lancet Digital Health*, 4(6):e406–e414, 2022.

Ben Glocker, Charles Jones, Mélanie Bernhardt, and Stefan Winzeck. Algorithmic encoding of protected characteristics in chest x-ray disease detection models. *EBioMedicine*, 89, 2023a.

Ben Glocker, Charles Jones, Mélanie Roschewitz, and Stefan Winzeck. Risk of bias in chest radiography deep learning foundation models. *Radiology: Artificial Intelligence*, 5(6):e230060, 2023b.

Patrick Godau, Piotr Kalinowski, Evangelia Christodoulou, Annika Reinke, Minu Tizabi, Luciana Ferrer, Paul Jäger, and Lena Maier-Hein. Navigating prevalence shifts in image analysis algorithm deployment. *Medical Image Analysis*, 102:103504, 2025. ISSN 1361-8415.

Hao Guan and Mingxia Liu. Domain adaptation for medical image analysis: a survey. *IEEE Transactions on Biomedical Engineering*, 69(3):1173–1185, 2021.

Xiaoyuan Guo, Judy Wawira Gichoya, Hari Trivedi, Saptarshi Purkayastha, and Imon Banerjee. Medshift: Automated identification of shift data for medical image dataset curation. *IEEE Journal of Biomedical and Health Informatics*, 27(8):3936–3947, 2023.

Moritz Hardt, Eric Price, and Nati Srebro. Equality of opportunity in supervised learning. *Advances in neural information processing systems*, 29, 2016.

Fereshteh Hasanzadeh, Colin B. Josephson, Gabriella Waters, Demilade Adedinsewo, Zahra Azizi, and James A. White. Bias recognition and mitigation strategies in artificial intelligence healthcare applications. *npj Digital Medicine*, 8(1):154, 2025. ISSN 2398-6352. doi: 10.1038/s41746-025-01503-7.

Clément Hognon, Pierre-Henri Conze, Vincent Bourbonne, Olivier Gallinato, Thierry Colin, Vincent Jaouen, and Dimitris Visvikis. Contrastive image adaptation for acquisition shift reduction in medical imaging. *Artificial Intelligence in Medicine*, 148:102747, 2024.

Sara Hooker. Moving beyond "algorithmic bias is a data problem". *Patterns*, 2(4), 2021.

Sara Hooker, Aaron Courville, Gregory Clark, Yann Dauphin, and Andrea Frome. What do compressed deep neural networks forget? *arXiv preprint arXiv:1911.05248*, 2019.

Sara Hooker, Nyalleng Moorosi, Gregory Clark, Samy Bengio, and Emily Denton. Characterising bias in compressed models. *arXiv preprint arXiv:2010.03058*, 2020.

Jeremy Irvin, Pranav Rajpurkar, Michael Ko, Yifan Yu, Silviana Ciurea-Ilcus, Chris Chute, Henrik Marklund, Behzad Haghgoo, Robyn Ball, Katie Shpanskaya, et al. Chexpert: A large chest radiograph dataset with uncertainty labels and expert comparison. In *Proceedings of the AAAI conference on artificial intelligence*, volume 33, pp. 590–597, 2019.

Ziheng Jiang, Chiyuan Zhang, Kunal Talwar, and Michael C Mozer. Characterizing structural regularities of labeled data in overparameterized models. *arXiv preprint arXiv:2002.03206*, 2020.

Alistair EW Johnson, Tom J Pollard, Seth J Berkowitz, Nathaniel R Greenbaum, Matthew P Lungren, Chih-ying Deng, Roger G Mark, and Steven Horng. Mimic-cxr, a de-identified publicly available database of chest radiographs with free-text reports. *Scientific data*, 6(1):317, 2019.

Charles Jones, Daniel C Castro, Fabio De Sousa Ribeiro, Ozan Oktay, Melissa McCradden, and Ben Glocker. No fair lunch: A causal perspective on dataset bias in machine learning for medical imaging. *arXiv preprint arXiv:2307.16526*, 2023.

Konstantinos Kamnitsas, Christian Baumgartner, Christian Ledig, Virginia Newcombe, Joanna Simpson, Andrew Kane, David Menon, Aditya Nori, Antonio Criminisi, Daniel Rueckert, et al. Unsupervised domain adaptation in brain lesion segmentation with adversarial networks. In *Information Processing in Medical Imaging: 25th International Conference, IPMI 2017, Boone, NC, USA, June 25-30, 2017, Proceedings 25*, pp. 597–609. Springer, 2017a.

Konstantinos Kamnitsas, Christian Ledig, Virginia FJ Newcombe, Joanna P Simpson, Andrew D Kane, David K Menon, Daniel Rueckert, and Ben Glocker. Efficient multi-scale 3d cnn with fully connected crf for accurate brain lesion segmentation. *Medical image analysis*, 36:61–78, 2017b.

Asal Khoshravan Azar, Barbara Draghi, Ylenia Rotalinti, Puja Myles, and Allan Tucker. The impact of bias on drift detection in ai health software. In *Artificial Intelligence in Medicine*, pp. 313–322, 2023. ISBN 978-3-031-34344-5.

Burak Koçak, Andrea Ponsiglione, Arnaldo Stanzione, Christian Bluethgen, João Santinha, Lorenzo Ugga, Merel Huisman, Michail E Klontzas, Roberto Cannella, Renato Cuocolo, et al. Bias in artificial intelligence for medical imaging: fundamentals, detection, avoidance, mitigation, challenges, ethics, and prospects. *Diagn Interv Radiol*, 2024.

Burak Koçak, Andrea Ponsiglione, Arnaldo Stanzione, Christian Bluethgen, João Santinha, Lorenzo Ugga, Merel Huisman, Michail E Klontzas, Roberto Cannella, and Renato Cuocolo. Bias in artificial intelligence for medical imaging: fundamentals, detection, avoidance, mitigation, challenges, ethics, and prospects. *Diagnostic and Interventional Radiology*, 31(2):75–88, 2025.

Lisa M Koch, Christian F Baumgartner, and Philipp Berens. Distribution shift detection for the postmarket surveillance of medical ai algorithms: a retrospective simulation study. *NPJ Digital Medicine*, 7(1):120, 2024.

Ali Kore, Elyar Abbasi Bavil, Vallijah Subasri, Moustafa Abdalla, Benjamin Fine, Elham Dolatabadi, and Mohamed Abdalla. Empirical data drift detection experiments on real-world medical imaging data. *Nature Communications*, 15(1):1887, 2024.

Matthew A Kupinski, John W Hoppin, Eric Clarkson, Harrison H Barrett, and George A Kastis. Estimation in medical imaging without a gold standard. *Academic radiology*, 9(3):290–297, 2002.

Mingxuan Liu, Yilin Ning, Salinelat Teixayavong, Mayli Mertens, Jie Xu, Daniel Shu Wei Ting, Lionel Tim-Ee Cheng, Jasmine Chiat Ling Ong, Zhen Ling Teo, Ting Fang Tan, et al. A translational perspective towards clinical ai fairness. *NPJ Digital Medicine*, 6(1):172, 2023.

William Lotter. Acquisition parameters influence ai recognition of race in chest x-rays and mitigating these factors reduces underdiagnosis bias. *Nature Communications*, 15(1):7465, August 2024. ISSN 2041-1723. doi: 10.1038/s41467-024-52003-3. URL https://doi.org/10.1038/s41467-024-52003-3.

Anant Madabhushi and George Lee. Image analysis and machine learning in digital pathology: Challenges and opportunities. *Medical image analysis*, 33:170–175, 2016.

Ricards Marcinkevics, Ece Ozkan, and Julia E Vogt. Debiasing deep chest x-ray classifiers using intra-and post-processing methods. In *Machine Learning for Healthcare Conference*, pp. 504–536. PMLR, 2022.

Amarachi B Mbakwe, Ismini Lourentzou, Leo Anthony Celi, and Joy T Wu. Fairness metrics for health ai: we have a long way to go. *EBioMedicine*, 90, 2023.

Jameson Merkow, Arjun Soin, Jin Long, Joseph Paul Cohen, Smitha Saligrama, Christopher Bridge, Xiyu Yang, Stephen Kaiser, Steven Borg, Ivan Tarapov, et al. Chexstray: a real-time multi-modal monitoring workflow for medical imaging ai. In *International Conference on Medical Image Computing and Computer-Assisted Intervention*, pp. 326–336. Springer, 2023.

Ibomoiye Domor Mienye, Theo G Swart, and George Obaido. Fairness metrics in ai healthcare applications: a review. In *2024 IEEE International Conference on Information Reuse and Integration for Data Science (IRI)*, pp. 284–289. IEEE, 2024.

Jose G Moreno-Torres, Troy Raeder, Rocío Alaiz-Rodríguez, Nitesh V Chawla, and Francisco Herrera. A unifying view on dataset shift in classification. *Pattern recognition*, 45(1):521–530, 2012.

Johanna P Müller and Bernhard Kainz. nnood: A framework for benchmarking self-supervised anomaly localisation methods. In *Uncertainty for Safe Utilization of Machine Learning in Medical Imaging: 4th International Workshop, UNSURE 2022, Held in Conjunction with MICCAI 2022, Singapore, September 18, 2022, Proceedings*, volume 13563, pp. 103. Springer Nature, 2022.

Nihal Murali, Aahlad Puli, Ke Yu, Rajesh Ranganath, and Kayhan Batmanghelich. Beyond distribution shift: Spurious features through the lens of training dynamics. *Transactions on machine learning research*, 2023, 2023.

Sergio Naval Marimont, Matthew Baugh, Vasilis Siomos, Christos Tzelepis, Bernhard Kainz, and Giacomo Tarroni. Disyre: Diffusion-inspired synthetic restoration for unsupervised anomaly detection. In *Proceedings/IEEE International Symposium on Biomedical Imaging: from nano to macro. IEEE International Symposium on Biomedical Imaging*. IEEE, 2024.

Ziad Obermeyer, Brian Powers, Christine Vogeli, and Sendhil Mullainathan. Dissecting racial bias in an algorithm used to manage the health of populations. *Science*, 366(6464):447–453, 2019.

Mahmud Omar, Shelly Soffer, Reem Agbareia, Nicola Luigi Bragazzi, Donald U. Apakama, Carol R. Horowitz, Alexander W. Charney, Robert Freeman, Benjamin Kummer, Benjamin S. Glicksberg, Girish N. Nadkarni, and Eyal Klang. Sociodemographic biases in medical decision making by large language models. *Nature Medicine*, 31(6):1873–1881, 2025. ISSN 1546-170X. doi: 10.1038/s41591-025-03626-6.

Roland Opfer, Julia Krüger, Lothar Spies, Ann-Christin Ostwaldt, Hagen H Kitzler, Sven Schippling, and Ralph Buchert. Automatic segmentation of the thalamus using a massively trained 3d convolutional neural network: higher sensitivity for the detection of reduced thalamus volume by improved inter-scanner stability. *European radiology*, 33(3):1852–1861, 2023.

Cheng Ouyang, Konstantinos Kamnitsas, Carlo Biffi, Jinming Duan, and Daniel Rueckert. Data efficient unsupervised domain adaptation for cross-modality image segmentation. In *Medical Image Computing and Computer Assisted Intervention–MICCAI 2019: 22nd International Conference, Shenzhen, China, October 13–17, 2019, Proceedings, Part II 22*, pp. 669–677. Springer, 2019.

Cheng Ouyang, Carlo Biffi, Chen Chen, Turkay Kart, Huaqi Qiu, and Daniel Rueckert. Self-supervised learning for few-shot medical image segmentation. *IEEE Transactions on Medical Imaging*, 41(7):1837–1848, 2022a.

Cheng Ouyang, Chen Chen, Surui Li, Zeju Li, Chen Qin, Wenjia Bai, and Daniel Rueckert. Causality-inspired single-source domain generalization for medical image segmentation. *IEEE Transactions on Medical Imaging*, 42(4):1095–1106, 2022b.

Yaniv Ovadia, Emily Fertig, Jie Ren, Zachary Nado, David Sculley, Sebastian Nowozin, Joshua Dillon, Balaji Lakshminarayanan, and Jasper Snoek. Can you trust your model's uncertainty? evaluating predictive uncertainty under dataset shift. *Advances in neural information processing systems*, 32, 2019.

Johanna P. Müller, Matthew Baugh, Jeremy Tan, Mischa Dombrowski, and Bernhard Kainz. Confidence-aware and self-supervised image anomaly localisation. In *International Workshop on Uncertainty for Safe Utilization of Machine Learning in Medical Imaging*, pp. 177–187. Springer, 2023.

Carolina Piçarra and Ben Glocker. Analysing race and sex bias in brain age prediction. In *Workshop on Clinical Image-Based Procedures*, pp. 194–204. Springer, 2023.

Esther Puyol-Antón, Bram Ruijsink, Stefan K. Piechnik, Stefan Neubauer, Steffen E. Petersen, Reza Razavi, and Andrew P. King. Fairness in cardiac mr image analysis: An investigation of bias due to data imbalance in deep learning based segmentation. In Marleen de Bruijne, Philippe C. Cattin, Stéphane Cotin, Nicolas Padoy, Stefanie Speidel, Yefeng Zheng, and Caroline Essert (eds.), *Medical Image Computing and Computer Assisted Intervention – MICCAI 2021*, pp. 413–423, 2021. ISBN 978-3-030-87199-4.

Joaquin Quiñonero-Candela, Masashi Sugiyama, Anton Schwaighofer, and Neil D Lawrence. *Dataset shift in machine learning*. Mit Press, 2022.

Stephan Rabanser, Stephan Günnemann, and Zachary Lipton. Failing loudly: An empirical study of methods for detecting dataset shift. *Advances in Neural Information Processing Systems*, 32, 2019.

Ricardo Trainotti Rabonato and Lilian Berton. A systematic review of fairness in machine learning. *AI and Ethics*, pp. 1–12, 2024.

Pranav Rajpurkar, Jeremy Irvin, Aarti Bagul, Daisy Ding, Tony Duan, Hershel Mehta, Brandon Yang, Kaylie Zhu, Dillon Laird, Robyn L Ball, et al. Mura: Large dataset for abnormality detection in musculoskeletal radiographs. *arXiv preprint arXiv:1712.06957*, 2017.

Mélanie Roschewitz, Galvin Khara, Joe Yearsley, Nisha Sharma, Jonathan J James, Éva Ambrózay, Adam Heroux, Peter Kecskemethy, Tobias Rijken, and Ben Glocker. Automatic correction of performance drift under acquisition shift in medical image classification. *Nature Communications*, 14(1):6608, 2023.

Johannes Rueckel, Lena Trappmann, Balthasar Schachtner, Philipp Wesp, Boj Friedrich Hoppe, Nicola Fink, Jens Ricke, Julien Dinkel, Michael Ingrisch, and Bastian Oliver Sabel. Impact of confounding thoracic tubes and pleural dehiscence extent on artificial intelligence pneumothorax detection in chest radiographs. *Investigative Radiology*, 55(12):792–798, 2020.

Berkman Sahiner, Weijie Chen, Ravi K Samala, and Nicholas Petrick. Data drift in medical machine learning: implications and potential remedies. *The British Journal of Radiology*, 96(1150):20220878, 2023.

Zohaib Salahuddin, Henry C Woodruff, Avishek Chatterjee, and Philippe Lambin. Transparency of deep neural networks for medical image analysis: A review of interpretability methods. *Computers in biology and medicine*, 140:105111, 2022.

Yash Savani, Colin White, and Naveen Sundar Govindarajulu. Intra-processing methods for debiasing neural networks. *Advances in neural information processing systems*, 33:2798–2810, 2020.

Shier Nee Saw and Kwan Hoong Ng. Current challenges of implementing artificial intelligence in medical imaging. *Physica Medica*, 100:12–17, 2022.

Hannah M Schlüter, Jeremy Tan, Benjamin Hou, and Bernhard Kainz. Natural synthetic anomalies for self-supervised anomaly detection and localization. In *European Conference on Computer Vision*, pp. 474–489. Springer, 2022.

Bernhard Schölkopf, Dominik Janzing, Jonas Peters, Eleni Sgouritsa, Kun Zhang, and Joris Mooij. On causal and anticausal learning. In *Proceedings of the 29th International Coference on International Conference on Machine Learning*, ICML'12, pp. 459–466, Madison, WI, USA, 2012. Omnipress. ISBN 9781450312851.

Bernhard Schölkopf, Dominik Janzing, Jonas Peters, Eleni Sgouritsa, Kun Zhang, and Joris Mooij. On causal and anticausal learning. *arXiv preprint arXiv:1206.6471*, 2012.

Andrew B Sellergren, Christina Chen, Zaid Nabulsi, Yuanzhen Li, Aaron Maschinot, Aaron Sarna, Jenny Huang, Charles Lau, Sreenivasa Raju Kalidindi, Mozziyar Etemadi, et al. Simplified transfer learning for chest radiography models using less data. *Radiology*, 305(2):454–465, 2022.

Laleh Seyyed-Kalantari, Guanxiong Liu, Matthew McDermott, Irene Y Chen, and Marzyeh Ghassemi. Chexclusion: Fairness gaps in deep chest x-ray classifiers. In *BIOCOMPUTING 2021: proceedings of the Pacific symposium*, pp. 232–243. World Scientific, 2020.

Laleh Seyyed-Kalantari, Haoran Zhang, Matthew BA McDermott, Irene Y Chen, and Marzyeh Ghassemi. Underdiagnosis bias of artificial intelligence algorithms applied to chest radiographs in under-served patient populations. *Nature medicine*, 27(12):2176–2182, 2021.

Agnieszka Słowik and Léon Bottou. Algorithmic bias and data bias: Understanding the relation between distributionally robust optimization and data curation. *arXiv preprint arXiv:2106.09467*, 2021.

Arjun Soin, Jameson Merkow, Jin Long, Joseph Paul Cohen, Smitha Saligrama, Stephen Kaiser, Steven Borg, Ivan Tarapov, and Matthew P Lungren. Chexstray: real-time multi-modal data concordance for drift detection in medical imaging ai. *arXiv preprint arXiv:2202.02833*, 2022.

Théo Sourget, Michelle Hestbek-Møller, Amelia Jiménez-Sánchez, Jack Junchi Xu, and Veronika Cheplygina. Mask of truth: Model sensitivity to unexpected regions of medical images. *Journal of Imaging Informatics in Medicine*, 2025. ISSN 2948-2933. doi: 10.1007/s10278-025-01531-5. URL https://doi.org/10.1007/s10278-025-01531-5.

Tamas Spisak. Statistical quantification of confounding bias in machine learning models. *Gigascience*, 11: giac082, 2022.

Karin Stacke, Gabriel Eilertsen, Jonas Unger, and Claes Lundström. Measuring domain shift for deep learning in histopathology. *IEEE journal of biomedical and health informatics*, 25(2):325–336, 2020.

Emma A M Stanley, Raissa Souza, Anthony J Winder, Vedant Gulve, Kimberly Amador, Matthias Wilms, and Nils D Forkert. Towards objective and systematic evaluation of bias in artificial intelligence for medical imaging. *Journal of the American Medical Informatics Association*, 31(11):2613–2621, 2024a. doi: 10.1093/jamia/ocae165.

Emma AM Stanley, Matthias Wilms, and Nils D Forkert. A flexible framework for simulating and evaluating biases in deep learning-based medical image analysis. In *International Conference on Medical Image Computing and Computer-Assisted Intervention*, pp. 489–499. Springer, 2023.

Emma AM Stanley, Raissa Souza, Anthony J Winder, Vedant Gulve, Kimberly Amador, Matthias Wilms, and Nils D Forkert. Towards objective and systematic evaluation of bias in artificial intelligence for medical imaging. *Journal of the American Medical Informatics Association*, pp. ocae165, 2024b.

Jeremy Tan, Benjamin Hou, Thomas Day, John Simpson, Daniel Rueckert, and Bernhard Kainz. Detecting outliers with poisson image interpolation. In *Medical Image Computing and Computer Assisted Intervention–MICCAI 2021: 24th International Conference, Strasbourg, France, September 27–October 1, 2021, Proceedings, Part V 24*, pp. 581–591. Springer, 2021.

Ali S Tejani, Yee Seng Ng, Yin Xi, and Jesse C Rayan. Understanding and mitigating bias in imaging artificial intelligence. *Radiographics*, 44(5):e230067, 2024.

Vanya V Valindria, Ioannis Lavdas, Wenjia Bai, Konstantinos Kamnitsas, Eric O Aboagye, Andrea G Rockall, Daniel Rueckert, and Ben Glocker. Reverse classification accuracy: predicting segmentation performance in the absence of ground truth. *IEEE transactions on medical imaging*, 36(8):1597–1606, 2017.

Sahil Verma and Julia Rubin. Fairness definitions explained. In *Proceedings of the International Workshop on Software Fairness*, FairWare '18, pp. 1–7, New York, NY, USA, 2018. Association for Computing Machinery. ISBN 9781450357463. doi: 10.1145/3194770.3194776. URL https://doi.org/10.1145/3194770.3194776.

Amey Vrudhula, Alan C. Kwan, David Ouyang, and Susan Cheng. Machine learning and bias in medical imaging: Opportunities and challenges. *Circulation: Cardiovascular Imaging*, 17(2):e015495, 2024.

Christian Wachinger, Benjamin Gutierrez Becker, Anna Rieckmann, and Sebastian Pölsterl. Quantifying confounding bias in neuroimaging datasets with causal inference. In *Medical Image Computing and Computer Assisted Intervention–MICCAI 2019: 22nd International Conference, Shenzhen, China, October 13–17, 2019, Proceedings, Part IV 22*, pp. 484–492. Springer, 2019.

Geoffrey I Webb, Roy Hyde, Hong Cao, Hai Long Nguyen, and Francois Petitjean. Characterizing concept drift. *Data Mining and Knowledge Discovery*, 30(4):964–994, 2016.

Jingkang Yang, Kaiyang Zhou, Yixuan Li, and Ziwei Liu. Generalized out-of-distribution detection: A survey. *International Journal of Computer Vision*, pp. 1–28, 2024a.

Yuzhe Yang, Haoran Zhang, Judy W Gichoya, Dina Katabi, and Marzyeh Ghassemi. The limits of fair medical imaging ai in real-world generalization. *Nature Medicine*, pp. 1–11, 2024b.

John R Zech, Marcus A Badgeley, Manway Liu, Anthony B Costa, Joseph J Titano, and Eric Karl Oermann. Variable generalization performance of a deep learning model to detect pneumonia in chest radiographs: a cross-sectional study. *PLoS medicine*, 15(11):e1002683, 2018.

Darko Zikic, Ben Glocker, and Antonio Criminisi. Encoding atlases by randomized classification forests for efficient multi-atlas label propagation. *Medical image analysis*, 18(8):1262–1273, 2014.

David Zimmerer, Peter M Full, Fabian Isensee, Paul Jäger, Tim Adler, Jens Petersen, Gregor Köhler, Tobias Ross, Annika Reinke, Antanas Kascenas, et al. Mood 2020: A public benchmark for out-of-distribution detection and localization on medical images. *IEEE Transactions on Medical Imaging*, 41(10):2728–2738, 2022.